Master's thesis

NTNU
Norwegian University of Science and Technology
Faculty of Medicine and Health Sciences
Department of Clinical and Molecular Medicine

Celia Torrado

Liquid biopsy in hematological cancers

Testing digital droplet PCR as a method for mutation detection in serum from Waldenstrom Macroglobulinemia, Hairy cell leukemia and Acute Promyelocytic Leukemia

Master's thesis in Biotechnology
Supervisor: Trygve Brautaset, Kristine Misund
June 2019

NTNU
Norwegian University of
Science and Technology

Celia Torrado

Liquid biopsy in hematological cancers

Testing digital droplet PCR as a method for mutation detection in serum from Waldenstrom Macroglobulinemia, Hairy cell leukemia and Acute Promyelocytic Leukemia

Master's thesis in Biotechnology
Supervisor: Trygve Brautaset, Kristine Misund
June 2019

Norwegian University of Science and Technology
Faculty of Medicine and Health Sciences
Department of Clinical and Molecular Medicine

NTNU
Norwegian University of
Science and Technology

Preface and acknowledgement

This master thesis was performed at the department of clinic and molecular medicine (IKOM) at the Norwegian University of Science and Technology (NTNU) in collaboration with St. Olav hospital and the biotechnology department at NTNU.

First of all, I would like to thank my supervisor Trygve Brautaset from the Biotechnology department for giving me the opportunity to carry out this thesis at the department of clinic and molecular medicine.

I would like to express my gratitude to my co-supervisor Kristine Misund for the engagement in this mater thesis, explanations, guidance, suggestions and comments through all this year.

I want also to thank Elisabeth Fritzke Emdal for all her help and patience in the lab showing me all the techniques, experimental work and experimental design. Thank you also for the contributions to the project and inputs during the writing process of the thesis.

Finally, I want to thank Anders Waage, for being part of the discussions and sharing his knowledge contributing to the most clinical aspects of the project. I am grateful for having had the chance to listen and learn from his experience.

Abstract

Circulating tumor DNA (ctDNA), isolated from plasma or serum, has been shown to be a good biomarker for many cancers. However, its detection can be challenging due to its low concentration in blood. In this project, serum ctDNA was used for the analysis of two point mutations, Myd88 L265P, present in Waldenstrom Macroglobulinemia (WM) and BRAF V600E in Hairy Cell Leukemia (HCL), and one translocation, PML-RARA in patients with Acute Promyelocytic Leukemia (APL). Digital droplet polymerase chain reaction (ddPCR) was chosen as the method for the detection of the mutations due to its high sensitivity and easy to use.

First, the validation of the 3 assays, Myd88 L265P, BRAF V600E and PML-RARA, was carried out. In the case PML-RARA, two transcripts were analyzed (Bcr1_2 and Bcr3). Myd88 and PML-RARA (transcript bcr1_2) assays showed a sensitivity of 0,05%, (mutant allele frequency) and BRAF and PML-RARA (bcr3) assays showed a lower sensitivity, around 0,15%. Secondly, eight patients with WM, one diagnosed with monoclonal gammopathy of undetermined significance and two with HCL were analyzed: Four of the WM patients were positive for the mutation, while three WM patients' results were unclear. The other two WM patients were negative for the mutation. Also, 19 time points form a WM patient were analyzed and compared with serum monoclonal IgM (used for disease monitoring in WM patients). The results showed a good correlation between both indicators. Regarding the two HCL patients tested, one was negative for the mutation and the other showed a few positive copies, however the last patient was considered negative based on the limit of detection of the assay.

In all patient the ddPCR results correlated well with the clinical data, in those with an active disease the mutation was clearly found meanwhile in patients with remission of the disease the mutation was found in a lower concentration (or not found). For the analysis of APL patients, cfRNA was used, experiencing some challenges with RNA stability.

In conclusion, the mutation Myd88 L265P was detected in ctDNA and it could be used as biomarker in WM patients, besides it seems to have a similar sensitivity to M component. More samples are needed to determine whether it ctDNA can be used for the detection of the BRAF in HCL patients. For PML-RARA, method optimization is needed if this assay is to be further tested.

Abbreviations List

APL	Acute Promyelocytic Leukemia
AS-PCR	Allele Specific – Polymerase Chain Reaction
ATRA	All-Trans Retinoic Acid
ATO	Arsenic Trioxide
BM	Bone Marrow
BTK	Bruton Tyrosine Kinase
CfDNA	cell free DNA
CTC	Circulating Tumor Cells
ctDNA	circulating tumor DNA
cfNA	circulating nucleic acids
ddPCR	digital droplet PCR
FISH	Fluorescence In Situ Hybridization
FPR	False Positive Rate
HCL	Hairy Cell Leukemia
HMP	Hematopoietic Multipotent Progenitor
HSC	Hematopoietic Stem Cell
Ig	Immunoglobulin
IL-1	Interleukin 1
LoD	Limit of Detection
LPL	Lymphoplasmacytic Lymphoma
MGUS	Monoclonal Gammapathia of Uncertain Significance
MM	Multiple Myeloma
MPP	Multipotent Progenitor
MRD	Minimal Residual Disease
NC	Negative Control
NCI	National Cancer Institute
NK	Natural killer
NTC	Non-Template Control
PB	Peripheral Blood
PC	Positive Control
REK	Regional Committees for Medical and Health Research Ethics
RQ-PCR	Real time Quantitative PCR)

TLR:	Toll Like Receptor
WHO:	World Health Organization
WM:	Waldenstrom Macroglobulinemia
WT:	Wild Type

List of figures

List of tables

Contents

1. Introduction

1.1 Cancer landscape

Cancer is a global disease and is the second leading cause of death in developed countries causing 9,6 million deaths in 2018 and 18,1 million incident cases. The number of new cases is expected to increase mainly due to aging population (1). In Norway, cancer took 10.944 lives in 2016 and the incidence in 2017 was 33.567 cases.

According with World Health Organization (WHO) cancer is a generic term for a broad group of diseases characterized by the growth of abnormal cells (neoplasia) due to different alterations. These alterations, called mutations can promote uncontrolled cellular proliferation and avoid growth suppression and cell death signals leading to the invasion of adjacent tissues and the spreading of tumor cells to other organs (2, 3).

Cancer is understood as a result of sequential acquisition of mutations (either spontaneous, also called de-novo mutations, or hereditary mutations) (4). These mutations can either occur in proto-oncogenes, genes in which gain of function mutations can cause the development of a tumor, or in tumor suppressor genes, in which loss of function mutations are the cause of tumor development (5). Mutations can be classified into different types such as, single nucleotide mutations, small insertions or deletions or mutations that affect the whole chromosome including big insertion/deletions or translocations between two chromosomes (5).

Some types of tumors contain different mutations forming different clones, that arise from one mutated cell that can develop into other sub-clones. These clones, genetically diverse, evolve due to genetic changes leading to mutations that can confer more advantages to the cell, and can be distributed across different locations or can appear at different stages of the disease (3). Thus, cancer should be understood as a molecularly dynamic disease, one of the possible causes for therapy resistance and relapse in patients (3, 6).

The tumors can be broadly classified in solid or liquid tumors. Solid tumors are defined by the National Cancer Institute as an abnormal mass of tissue that usually does not contain cysts or liquid areas. However, liquid tumors, known as hematological malignancies involve blood cells and generally do not form solid tumors such as, myelomas and leukemias and lymphomas (7).

1.2. Hematological disorders

In 2018, 1,3 million people were living with any kind of hematological malignancy. 50% of hematological disease were diagnosed in population older than 65 years (8). In Norway, the incidence of the hematological malignances in 2017 was 2761 representing a 8% of all cancer incidents (9).

The formation of blood cells is known as hematopoiesis, (Figure 1) and it mainly takes place in bone marrow although some cells achieve their final maturation in other locations such as in peripheral blood or thymus (10). All blood cells derive from a common progenitor, the Hematopoietic Stem Cell (HSC). Numerous signaling molecules such as cytokines, hormones, transcription factors or prostaglandins drive the differentiation and maturation of the HSC into the hematopoietic multipotent progenitor (HMP). The HMP can be differentiated into 2 major progenitors: lymphoid progenitor that will lead to the lymphoid lineage and myeloid progenitor, leading to myeloid lineage. From the common lymphoid progenitor all types of lymphocytes are form, including Natural Killer cells, B and T lymphocytes (11, 12).

- **Natural killer cells:** its development and all steps of maturation are carried out in the bone marrow. These cells are in charge of mediating immunomodulatory effects (13)
- **B lymphocytes:** the development of B lymphocytes begins when the cell Pro-B starts several steps of rearrangement of Immunoglobulin (Ig) genes. As a result, the heavy chain of IgM (μ) is formed and the cell is called now Pre-C. Again, after several rearrangement steps and survival signals, the rest of the chains are formed and the lymphocyte become mature. The last step of differentiation of B cells is into plasma cells, cells that after the stimulation with a specific antigen will secrete one specific antibody in large amounts (14). These cells have a key role in humoral immune response by the production of immunoglobulins (Ig).
- **T lymphocytes** development and maturation occurs in the thymus. Similar to B cells, Pro-T cells undergo several steps of immunoglobulin genes rearrangement to end up with maturation of the lymphocyte. T cells are involve in the maintenance of the immune response, immunological memory and self-tolerance (15).

The cells that derive from the common myeloid progenitor are:

- **Megakaryocytes**: will end up generating thrombocytes, that together with coagulation factors act forming blood clots.

- **Erythroblast** that will be derived in erythrocytes and in charge of the oxygen transport
- **Monoblast** and **myeloblast** lead to macrophages and granulocytes and have also role in the immune system response against infections (10).

Dendritic cells can be derived from both lymphoid and myeloid precursor and have a key role as cell presenting antigens (10).

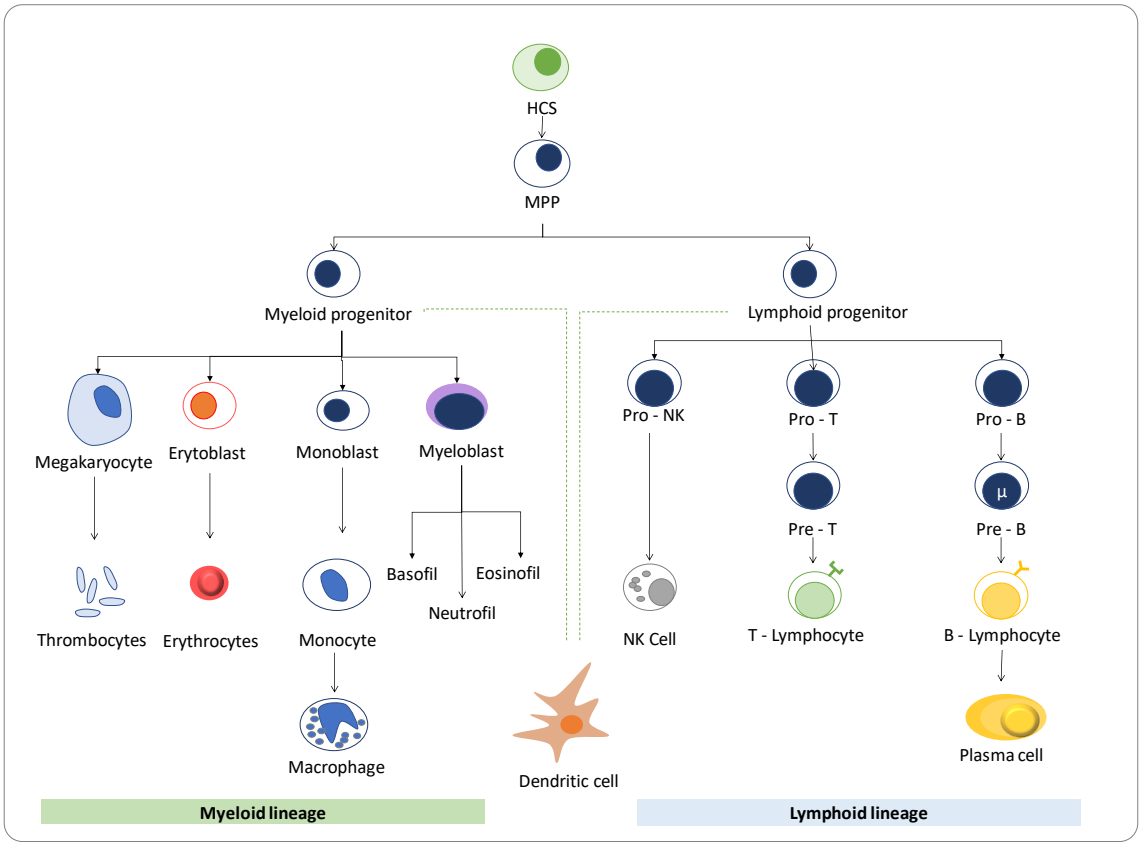

Figure 1 Hematopoiesis. Blood cell formation takes place mainly in bone marrow. In some cases, such as for plasma cells or T cells the last steps of maturation take place in the secondary lymphoid organs such as spleen or thymus. NB: This is a simplified figure; the hematopoiesis process is more complex and involve more steps. HCS: hematopoietic stem cell; MPP: multipotent progenitor; NK: natural killer (11, 15)

Mutations in blood cells occur at different stages of their development impeding the transition of the cell to a more mature stage. In many cases the mutations occur in the precursor cells and they are arrested in very un-developed stages.

Hematological malignancies can be classified into three categories according to which localizations of the body are involved: leukemia, lymphoma and myeloma. These three groups can be sub-classified depending on the lineage of the cell type from which the malignancy arise: myeloid lineage or lymphoid lineage (16). Figure 2 shows this classification that it will be further explained below:

- **Leukemias** → Leukemia begins in the bone marrow and the cancerous cells can be released into the blood stream. The different types of leukemias can arise from the 2 lineages lymphoid or myeloid Figure 3.
  - Myeloid lineage → The cells affected derived from the myeloid progenitor such as monoblast, myeloblast, megakaryocytes. This group include diseases such as Acute Promyelocytic leukemia, Chronic Myeloid Leukemia or Polycythemia Vera
  - Lymphoid lineage → The cells involved derived from the lymphoid progenitor such as B cells or T cells. This group includes Hairy cell leukemia or Acute lymphocytic leukemia
- **Lymphomas** → Lymphoma starts in the lymphatic system/node, so the cells tend to aggregate and form solid tumors in lymphatic tissues. There are 2 major types, Hodgkin, less common and characterized by the presence cells called Reed-Sternberg cells and Non-Hodgkin, more common and includes many malignancies. Lymphomas can arise only from the lymphoid lineage.
  - Lymphoid lineage → Cells involved are those from the lymphoid lineage such as B cells or T cells. Some examples of malignancies in this group are Lymphoplasmacytic lymphoma – Waldenstrom Macroglobulinemia (WM), Burkitt lymphoma or Anaplastic large cell lymphoma
- **Myeloma** → The most common type of myeloma is Multiple Myeloma (MM) (90% of the cases), other types of myeloma are: Plasmacytoma and Extramedullary myeloma. Multiple myeloma has its origin in bone marrow and arise from the plasma cells (Figure 2). It is characterized by clonal proliferation of plasma cells in the bone marrow and secretion of a monoclonal Ig due to the proliferation of a single clone of plasma cells. It is thought that this disorder can evolve from a precursor stage called monoclonal gammopathy of undetermined significance (MGUS) (17).

However, in many cases the origin of the hematologic cancer is unclear and, in some cases, it is ambiguous and more than one stage of development can be involved (18).

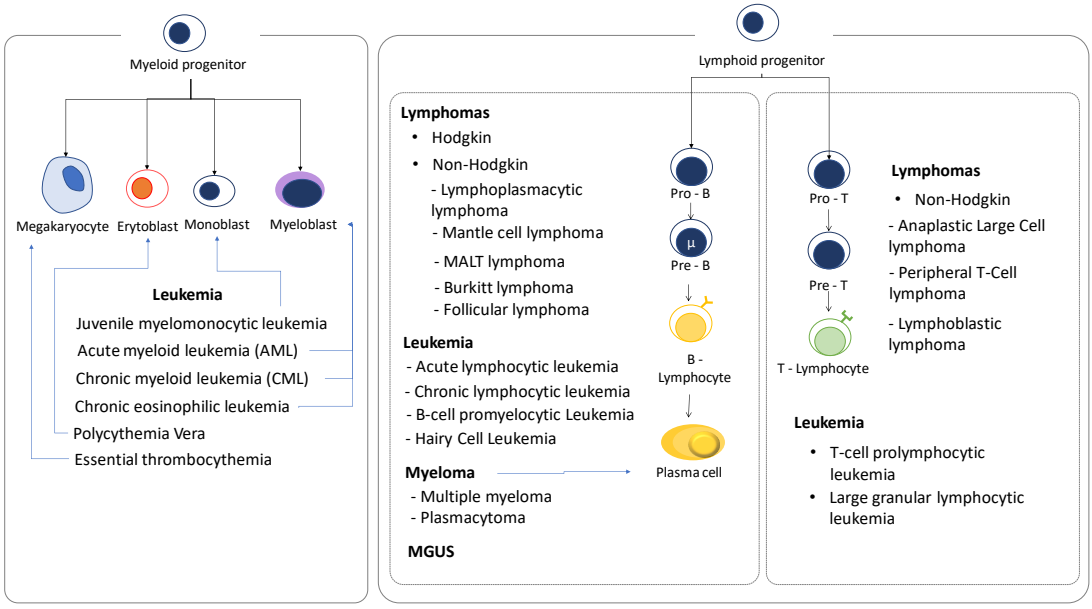

Figure 2 Haematological malignancies. Classification according to the three main groups; leukemia, lymphoma and myeloma and cell type form which the disease arises. Blue arrows show the cell type/stage that origin a specific disease. (19, 20).

1.3. Diseases

In this project, three hematological disorders are analyzed: Waldenstrom Macroglobulinemia (WM), Hairy Cell Leukemia (HCL) and Acute Promyelocytic Leukemia (APL), which are described more in detail.

1.3.1 Waldenstrom Macroglobulinemia

Waldenstrom Macroglobulinemia accounts for the 2% of all hematological neoplasia and is classified as a non-Hodgkin lymphoma of B cell, more in detail, is a type of lymphoplasmacytic lymphoma (Figure 2) (18, 21). It is thought that the individuals have a genetic susceptibility for the development of the malignancy and strong familial aggregation (22). WM is characterized by bone marrow infiltration of monoclonal lymphocytes, lymphoplasmacytic and plasma cells, and the presence of M component, monoclonal IgM – tumoral marker (23, 24). Although it is not well known from which stage of the B cell development WM arise from, it is thought that its origin is immature or mature B lymphocytes (Figure 3) (18). Cancer cells are mainly arrested in BM and sometimes are located in the glands, allowing its release to the blood stream. Most common clinical manifestations and symptoms are hepatomegaly, splenomegaly, anemia, hyper viscosity syndrome and anomalies in bleeding and clotting.

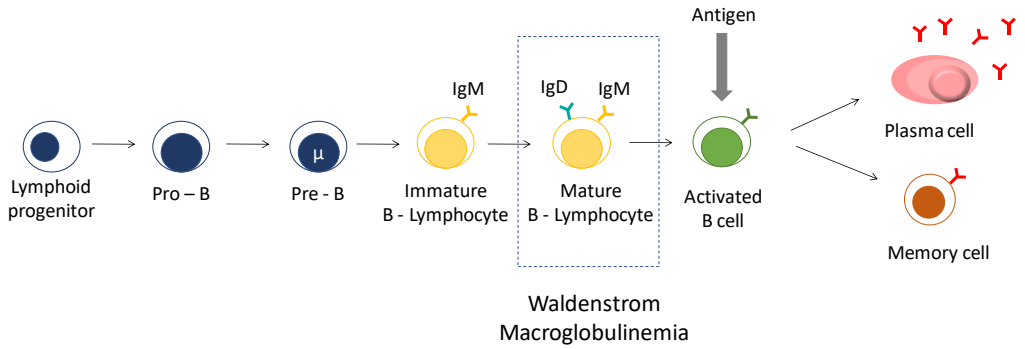

Figure 3 Stages of B-cell development. Detailed B cell formation

Regarding the molecular aspects of the disease, Treon et al. (25) described in 2012 that the mutation Myd88 L265P was present in 90% of the patients with WM, leading to new areas of research for both, the diagnosis and the treatment of the disorder (22, 25). Less common mutations in other genes have been found to be involved in the development of WM such as nonsense and frameshift mutations in the gen CXCR4 (mutated in 30% of the cases) (1, 6). This gene encodes for a chemokine receptor and has a role in immune response. The gene Myd88 is located in the short arm of chromosome 3 at position 3p22.2 and it's expressed in bone marrow and lymphoid node among others tissues (26, 27). Myd88 encodes for an adapter protein that is involved in the immune response, it functions as a signal transducer in the interleukin 1 (IL-1) and toll receptor (TLR) pathways (Figure 4). These pathways are involved in the activation of numerous proinflammatory genes.

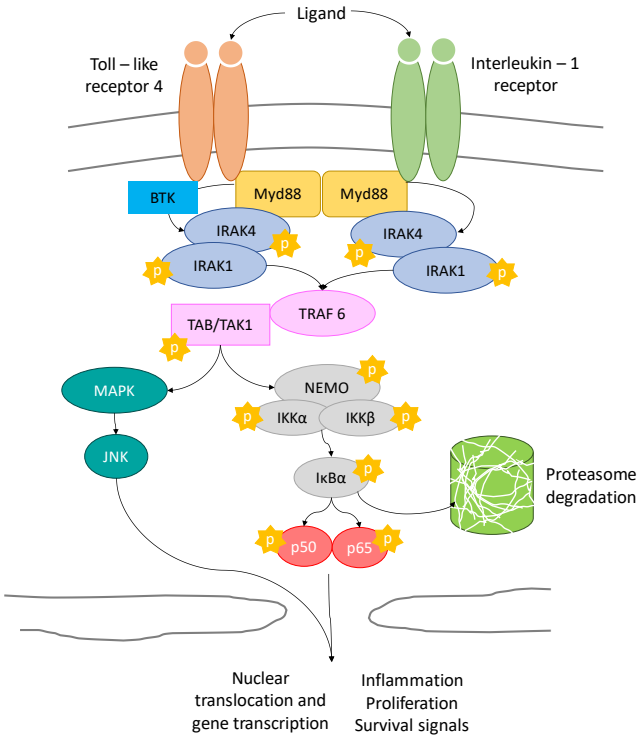

Figure 4. Toll like receptor and interleukin 1 signalling pathway. After the ligand binds the toll- like or the interleukin 1 receptor, the dimerization of Myd88 takes place and triggers the phosphorylation of IRAK4 through BTK (Bruton tyrosine kinase). Subsequently several signalling molecules are recruited and phosphorylated in a kinase cascade. The phosphorylation of these molecules leads to the activation and release of NF-kB p65 and p50 which translocate into the nucleus resulting into the transcription of inflammatory and survival genes. Besides, the TGF-β–activated kinase 1, TAK1 can activate MAP kinase pathway - Jnk (29). [Adapted from (25, 28)]

Gain of function mutations in Myd88, as is in the case of WM, activate downstream signaling pathways, and therefore, even in the absence of ligand the pathway remains active leading to abnormal overexpression of survival genes (28).

The Myd88 L265P mutation is a change of a single nucleotide T → C at position 978 (transcript NM_002468.4), switching from the trinucleotide CTG to CCG and leading to the change of the amino acid leucine for a proline in position 265 (L265P) (25, 29).
In the appendix, Figure 1S and Figure 2S there is a view of the sequence of the mRNA and the amino acid sequence of the protein and the mutation site.

MGUS

It is though that some WM patients can evolve from a pre-malignant stage, MGUS, Monoclonal gammopathy of undetermined significance. MGU is usually found in around 3% of healthy individuals over 50 years old. The most common gammopathy is IgG

followed by IgM. There is a risk of progression to a malignant disease such as multiple myeloma or Waldenstrom Macroglobulinemia (17, 21). It has been seen that 50% of the IgM MGUS carry the mutation Myd88 L265P and that around 15% carry the mutation CXCR4, this last mutation is thought to represent a progression factor of MyD88-mutated individuals to WM disease (21).

Diagnosis of WM requires the detection of IgM monoclonal protein in blood and at least 10% of lymphoplasmacytic lymphoma cells (LPL) (cells with characteristics of both, lymphocytes and plasma cells) in bone marrow (22, 23). However, the secretion of IgM is not equal in all tumors/patient and is not specific of WM but it is also present in other disorders such as MGUS, or multiple myeloma (IgM myeloma represent less than the 0.5% of all multiple myeloma cases(30)) (23). So far, the detection of LPL in bone marrow is necessary for the differential diagnosis between WM and MGUS. Besides, although the detection of the mutation Myd88 L265P is not in the clinical routines for the diagnosis of the disease it could be used for the differential diagnoses with WM and myeloma, since this mutation is not present in any MM patient (21). Moreover, one of the recommendations for the diagnosis of WM when a case is histopathologically difficult to interpret it the detection of the mutation Myd88 L265P by AS-PCR (allele specific – polymerase chain reaction) (22).

Treatment of WM patients starts when the disease become symptomatic, thus, patients with asymptomatic disease are only monitored until they show the first symptoms (22). The standard therapy for WM patients is rituximab combined with chemotherapy. Ibrutinib is given without chemotherapy and to all relapsed patients (22).

From the point of view of the genetic mutations, WM can be classified under 3 genotypes (21):

- Genotype 1: MYD88 mutated/CXCR4 wild-type
- Genotype 2: MYD88 mutated/CXCR4 mutated
- Genotype 3: MYD88 wild-type/CXCR4 wild-type

It has been seen that each genotype responds different to the different therapies, for instance the mutation CXCR4 confers resistance to ibrutinib. Patients with relapse and genotype 1 respond better to ibrutinib treatment compared with the other genotypes. Thus, knowing the molecular aspects of each patient could help for the management of the

disease. This disease remains incurable and it has a high percentage of relapse (22, 23). The median survival rate of patient after treatment has started is more than 6 years (23).

1.3.2. Hairy Cell Leukemia

Hairy Cell Leukemia is a rare, chronic B-cell lymphoproliferative disorder that accounts for 2% of all leukemias (31) and is classified as a leukemia that arise from the lymphoid lineage (Figure 2). It is known that HCL origin is in bone marrow and is developed from mature B cells (Figure 5). Some of the clinical symptoms are splenomegaly, pancytopenia and "hairy cells" (cells with a special morphology, small projections in the surface) infiltrating bone marrow, spleen, and peripheral blood (PB) (32).

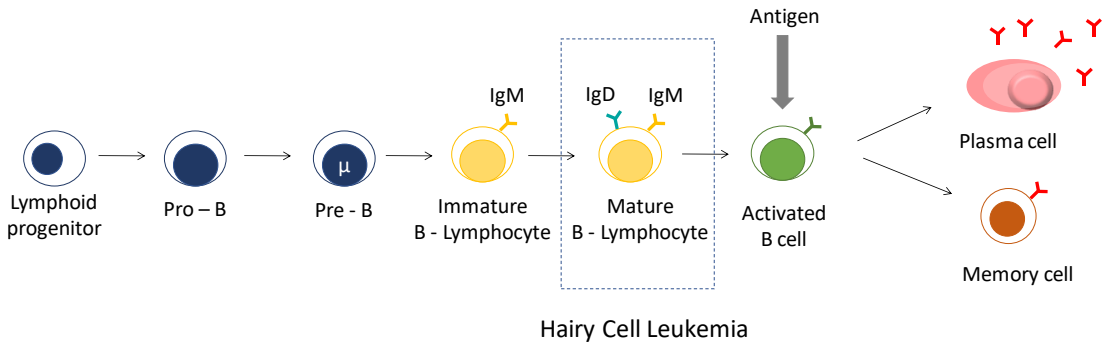

Figure 5 Stages of B-cell development.

The mutation found in nearly 100% of the HCL patients is BRAF V600E. This mutation first described by Triacci in 2011 (33) is already present in the HSC and in the lymphoid progenitor (34). Moreover, other genes have been reported to be mutated in HCL patients, such as the gene KLF2 or the tumor suppressor gene CDKN1B (p27) (31, 35).

BRAF gene is located in chromosome 7q34, and encodes for a protein kinase that belongs to the RAF family. This protein is involved in the MAP kinase signaling pathway that finalized with the activation of transcription factors important for proliferation, growth, survival and anti-apoptotic effects (36). Figure 6 shows MAP kinase signaling pathway.

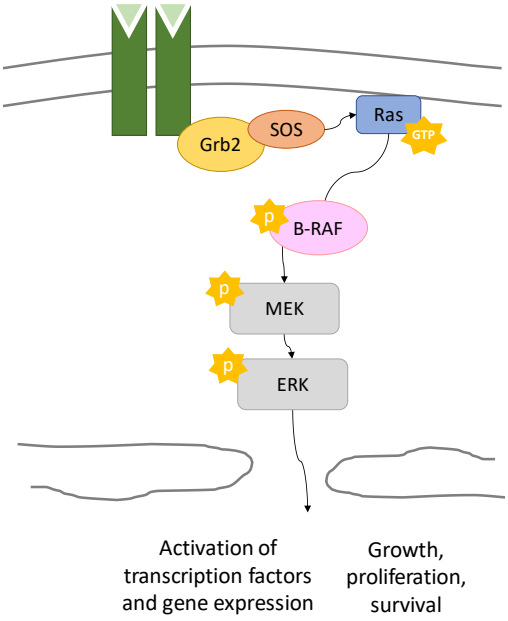

Figure 6 MAP kinase signalling pathway. After the ligand binds the receptor, it dimerized and several adaptor molecules are recruited (Grb2 and SOS). These molecules allow the activation of RAS by a change of GDP to GTP. RAS finally activates BRAF, and a kinase cascade starts with the phosphorylation and activation of the other kinases in the cascade (MEK and ERK). Finally, ERK is translocated to the nucleus where it activates several transcription factors [Adapted from (36)].

Several mutations have been found in BRAF, however, as mentioned before, BRAF V600E is the most common mutation (36). The switch of a single nucleotide T –> A at position 1799 (transcript NM_004333.4) leads to the mutation V600E, where an amino acid Valine is changed to Glutamate in position 600. Glutamate is electrically negatively charged, different from Valine that is a hydrophobic amino acid. It is though that Valine keeps BRAF inactive through hydrophobic interactions, and therefore, the change to Glutamate disrupt the hydrophobic interactions leading to an increase of the kinase activity and a constitutive activation of the MAP kinase signaling pathway (34, 37). Figure 3S and Figure 4S of the supplementary material, shows the sequence of the mRNA and the BRAF protein and the mutation site.

Diagnosis. The median age of diagnosis is 55 years old (31). This disease is diagnosed usually based on the detection of “Hairy cells” (cells with a specific morphology characteristic of the disease) and flow cytometry of a bone marrow biopsy detecting specific B cell markers such as CD25, CD23 or CD103. Although the detection of the mutation is not used in the clinical diagnosis, it is recommended for relapse and refractory patients, since the presence of the mutation can be used as therapeutic target. Moreover, there is a variant of HCL, named as HCL-v that lacks the BRAFV600E, thus, this

mutation could be useful for the differential diagnosis of these two malignancies (31, 34). Besides, some of the clinical symptoms of HCL such as splenomegaly, circulating leukemic cells or cytopenia are similar to other B cell malignancies such as splenic marginal zone lymphoma or diffuse small B cell lymphoma. In order to distinguish them from HCL, it may be useful the detection of the mutation BRAF V600E (35).

Treatment: Treatment starts with the presence of at least cytopenia (low count of neutrophil), a low hemoglobin level or a low count of platelet. Standard treatment with purine analogues (that will reduce DNA synthesis) is the first choice for HCL patients. In general, the disease has a good prognosis and most of the patients around 85% achieve a complete remission (35).The patients are not cured but the good response to treatment make the patients to remain in remission for several years. The median free survival after this treatment is more than 10 years (34). The discovery of this mutation allowed the improvement of the therapy, bringing up target therapy with kinase inhibitors drugs. Treatment with these inhibitors such as vemurafenib showed good response in many patients with relapse (34). Besides, mutations in other genes such as IRS1, NF1 or NF2 have been seen to be resistant to vemurafenib. Thus the detection of these mutations by a sensitive technique can be helpful for the choice of treatment for the patient (31).

1.3.3. Acute promyelocytic leukemia

Acute promyelocytic leukemia is a rare disorder classified by the WHO as sub-type of Acute Myeloid Leukemia (AML), 10% of AML cases. AML represent the 80% of the cases of leukemia in adults (38, 39). AML is a malignancy characterized by clonal expansion of myeloid blast (Figure 2) in bone marrow, peripheral blood, liver and spleen, that can result in severe leukocytosis and hemorrhage (39, 40). The French-American-British classification of leukemia divided this group into 8 sub-types depending the cell type from which the disease arise and its stage of maturation. Thus, APL is classified as M3 subtype and arise from the immature precursor promyelocyte (Figure 7) (41).

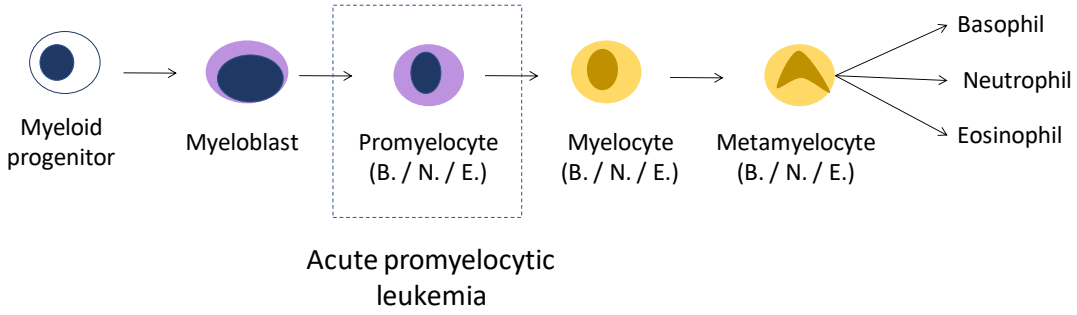

Figure 7 Stages of myeloblast development. Promyelocytes are developed from myeloblast, and there are three types B. N. and E. that will lead to the different cell types, Basophil (B), Neutrophil (N) and Eosinophil (E).

The molecular aberration involved in almost 90% of the cases is a reciprocal translocation between the genes PML and RARA, chromosomes 15 and 17 t(15;17)(q24;q21) (42, 43). PML in chromosome 15 (15q24.1) codes for a protein that belongs to the TRIM (tripartite motif) family. This protein is found in the nucleus of cells and functions as a transcription factor and tumor suppressor and has a role in the cell cycle and p53 regulation (44).

The second gene involved in the translocation is RARA in chromosome 17 (17q21.2), it codes for the retinoic acid receptor alpha (RAR), a nuclear receptor. This receptor regulates gene transcription according to the presence of ligand (retinoic acid) and is involved in processes such as cell development, differentiation and gene transcription (45). The retinoic acid pathway is shown in Figure 8.

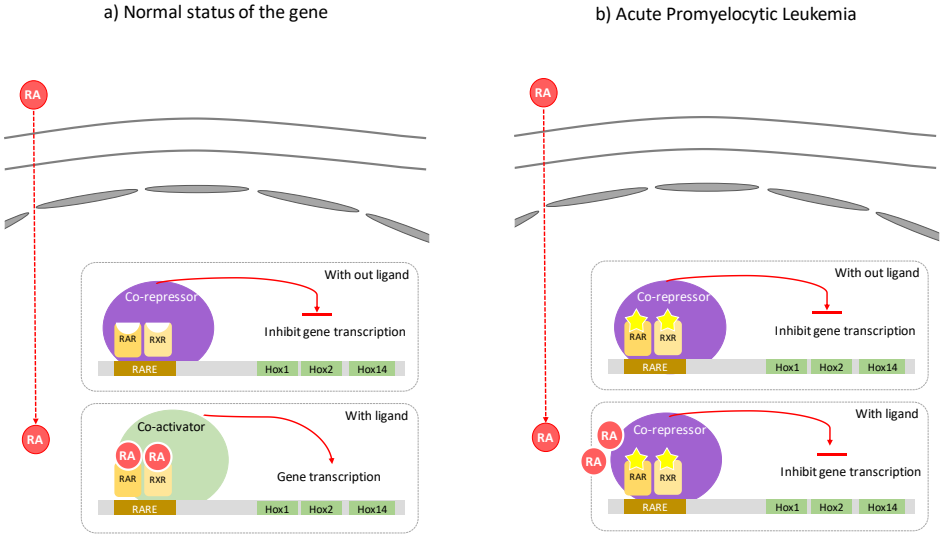

Figure 8 Retinoic acid signalling pathway. a) In the normal form of the gene, in the absence of ligand RA, the receptors RAR and RXA are bound to co-repressors resulting in the inhibition of gene transcription. When RA enter into the nucleus, it binds to the receptor resulting in the release of the co-repressors and co-activators are bound allowing gene transcription. **b)** In APL, the oncogenic fusion transcript resulting from

the translocation, PML-RARA, codes for an aberrant receptor that is no longer responsive to physiological RA signal, thus, even in the presence of RA the co-repressors remain bound to the receptor and gene transcription and other non-genomic activations doesn't take place, leading to myeloid precursors be arrested at the promyelocytic stage of maturation (48) [Adapted from (46)].

The translocation has different breaking points leading to different transcripts (Figure 9). The RARA gene has only one breaking point located in intron 2,), meanwhile gene PLM has three breaking points, leading to the transcripts bcr1, breaking point in intron 6; bcr2, breaking point in exon 6 and bcr3, breaking point in intron 3. (40, 42, 47).

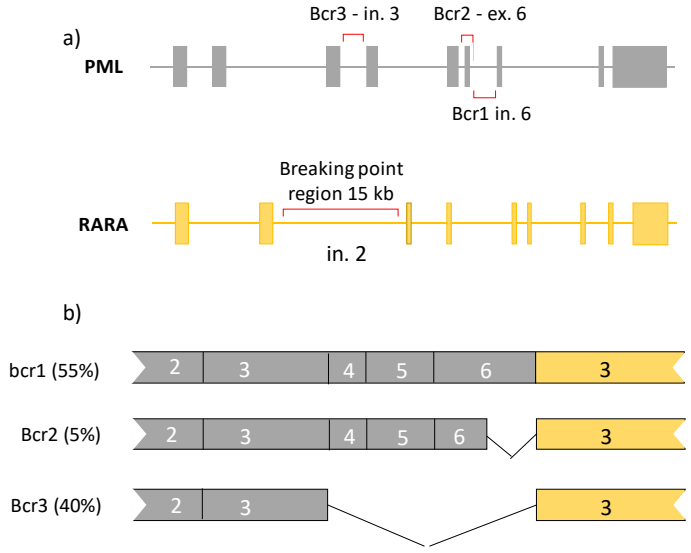

Figure 9. PML-RARA transcripts and breaking points. a) PML have three small break point cluster regions (bcr): bcr1 in intron 6, bcr2 in exon 6 and bcr3 in intron 3. In the RARA gene the break points cluster in intron 2. b) The three transcripts that results from the different breaking points. In parenthesis, the chance of occurrence. **[**Adapted form (47)]

Diagnosis of APL involve morphologic analysis (such as white blood cells count) and genetic test. The detection of the translocation is mandatory to confirm the diagnosis of the disease**.** FISH (fluorescence in situ hybridization) and RT-PCR (real time – PCR) are the main methods for its detection. Monitoring of the fusion transcript PML-RARA through RQ-PCR (real time quantitative PCR) is implemented in the clinical practice, mainly in patients with relapse in order to quantify the number of transcripts (48).

Treatment: In APL patients, the early diagnosis and early start of treatment is key for the prognosis of the patient due to the high risk of early death (20%) if the treatment is not given on time and high chances of cure (80%) when the treatment is given in advance (48). The standard treatment of APL is ATRA (all-trans retinoic acid) and ATO (arsenic trioxide). The treatment with ATRA and ATO has a high successful rate, achieving a

molecular remission of the 90-99% in the majority of the patients and their cure. Patients have low risk of relapse after treatment. These two drugs, target PML-RARA fusion transcript and its main mechanism of action is to degrade or break PML-RARA transcripts resulting in the decrease of leukemic blast (48) as well as remove the co-repressors that maintain the transcription factor inhibited (49). Since the main treatment of the disease is directly related to the translocation, its early detection is important for the success of the treatment and prognosis of the disease.

1.4. Liquid biopsy. Cell free nucleic acids and circulating tumor nucleic acids

The conventional biopsies, mainly surgical procedures and bone marrow samples are invasive, expensive, painful, can lead to numerous complications and sometimes cannot be performed if the tumor is inaccessible (50). New aproaches have arisen mainly based on the detection of components derived from the cancer, such as circulating tumor cells (CTC), exomes, miRNA or ctDNA (51).

Circulating cell free DNA (cfDNA) is formed by small DNA fragments, around 160 to 180 base pairs, that are released into the blood stream. The mechanisms by which these fragments are released are still no well-defined but it is thought that active transport, necrotic and/or apoptotic processes are the main mechanism (52, 53).

In 1997, Lo et at demonstrated the presence of cell circulating fetal DNA in the plasma of pregnant women having a great impact in pre-natal diagnosis (54). Despite the fact that cfDNA was discovered decades ago (1948 by Mandel and Metais) (55) its interest has increased the last years after it was demonstrated that the concentration of cfDNA was higher in certain pathological conditions, such as cancer. It has been demonstrated also that the concentration was even higher in those patients with advanced stage of the disease, leading to the idea that the release of cfDNA was more active in tumor cells (53). Cell free DNA released from tumor cells is called circulating tumor DNA (ctDNA). Moreover, it was shown that the ctDNA carried the same molecular profile as the tumor itself (53, 54). This led to the concept of liquid biopsy, a non-invasive quick and painless technique with low complications alternative to solid biopsy that allows the analysis of DNA fragments in blood (53, 54). Liquid biopsy can represent also a better view of the genetic heterogenicity of the different subclones of the cancer (53).

However, one of the drawbacks of the circulating nucleic acids is that its concentration in blood is quite low and varies between different individuals (both sick and healthy). It can vary from a few ng per ml of sample to thousands of ng per ml of sample depending the individual and the pathology (54). Besides, in cancer patients only a subset of the cfDNA is ctDNA (from 1% to 10% , depending of the tumor burden, out of the total of cfDNA, (50, 56)), requiring the use of sensitive methods for its detection.

When analyzing circulating free nucleic acids, it is possible to extract them from serum or plasma. Plasma is the liquid fraction of the blood resulting after blood centrifugation. Serum is the liquid fraction of the blood that results after its coagulation. Figure 10.

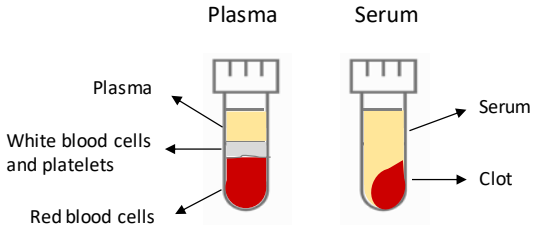

Figure 10 Plasma vs serum

Some studies have shown that the concentration of cfDNA is higher in serum than in plasma. However, during the clotting process in serum, some white blood cells can lyse resulting in the released of genomic DNA. Thus, plasma is considered a better source for cfDNA (54).

1.4.1 cfRNA and ctRNA

As well as cfDNA, molecules of RNA are found in peripheral blood. It can be found in different forms: microRNA, embed in vesicles such as exomes or microvesicles or free RNA molecules. It is believed that the mechanisms by which RNA is released are the same as for cfDNA and it seems to be also disease-dependent (57). Moreover, cfRNA analysis appear to be promising especially for the detection of fusion transcripts and splice variants (58). However, it has been described in many studies that one of the drawbacks of cfRNA is its instability due, in part, to the presence of RNases, making RNA easily degraded (57, 59). It has been seen that some proteins such as HDL, NPM1 or Ago1 bind and protect miRNA from endogenous RNAases activity (57). RNA in exomes or vesicles seem to have a higher protection against RNAases (58).

To conclude, liquid biopsy, and more specifically, ctDNA analysis is a promising technique that can give information about the tumor burden, detection of the mutations presents in the tumor, detection of minimal residual disease (MRD) or follow up and monitoring of treatment response (50, 60).

1.5. Digital Droplet PCR

Since ctDNA constitutes a small part of the total DNA circulating in the blood stream (1-10% (50)) , the detection of such DNA must be highly sensitive. Thus, a sensitive tool needs to be used for the accurate quantification of those DNA fragments.

Digital droplet PCR (ddPCR) is able to identify and quantify a single nucleotide mutation from non-mutated molecules which has higher abundance in a sample.

Among the different types of PCR, digital PCR provides an absolute quantification of the target sequence with high precision and high sensitivity (61). Digital PCR is able to reach a high sensitivity, thanks to the partitioning of the sample into thousands of simultaneous PCR reactions, the main principle of Digital PCR (Figure 11). The compartmentalization of the sample avoids the challenge of having a low frequent mutant in a high wild type background by distributing the background into the different droplets/wells and thus, reducing it in each individual PCR reaction. Many of the reactions will contain no target molecules, but those that contain a target will have lower competing background compare to that of the original sample (62).

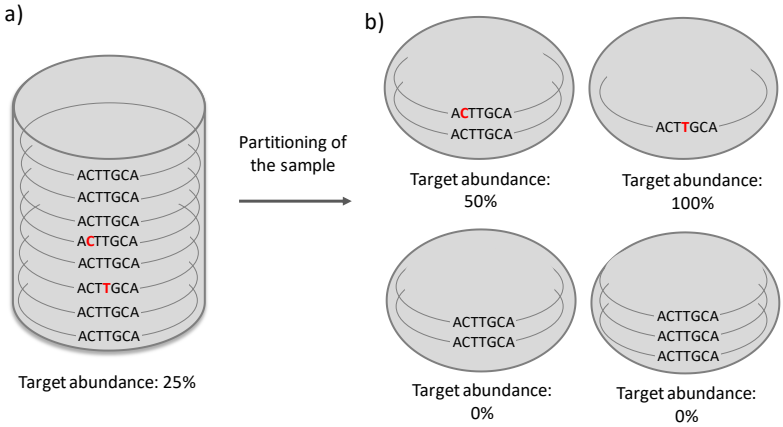

Figure 11. Main principle of Digital PCR. Partitioning of the sample. Target abundance is calculated as the mutant molecules out of the total of molecules. A) shows the original sample without partitioning, in. It can be seen how the mutant targets (in red) are surrounded by high amounts of WT molecules, making

difficult the detection of the mutant. b) the sample has been partitioning, resulting in the reduction of the background in each reaction, and thus, increasing the target abundance (63).

Several digital platforms have been designed such as, the QuantStudio 3D Digital PCR System (Thermo Fisher) and Droplet Digital PCR (Bio-Rad) among others. This master thesis experiments will be carried out using QX200™ Droplet Digital™ PCR platform.

Minimal residual disease has been already assessed successfully in other hematological malignancies and other solid tumors using ddPCR such as chronic myeloid leukemia involving BCR-ABL fusion gene, myeloproliferative neoplasms or prostate cancer among others (64-67).

2. Objectives

The Janus serum biobank in Norway has 318.628 serum samples reserved for cancer research. Samples from healthy donors started to be collected periodically from 1972 until 2004. It is known that around 25% of those healthy donors (84.043) ended up developing cancer (68).

In this thesis, the focus was on three cancer diseases, Waldenstrom Macroglobulinemia (WM), Hairy Cell leukemia (HCL) and Acute Promyelocytic Leukemia (APL), these three diseases have either a mutation (WM and HCL) or a translocation (APL) present in almost all of the patients (>90% of patients).

It is of huge biological interest to know how long the preclinical phase is for these diseases and to know how early are actually the mutations, and thus, the cancer cells, arising in an individual, later developing cancer.

The amount of serum in the samples in the Janus biobank is limited (max 0.5 ml), so there are several things that have to be tested before starting to analyze such samples, which will be the main aims for this work

1. Validate the 3 ddPCR assays, MYD88 L265P (WM disease), BRAF V600E (HCL disease), PML-RARA (APL disease) to see if the mutation can be detected by assessing the Limit of Detection (LoD) of each assay as well as the False Positive Rate (FPR)
2. Test patient serum samples from active disease stage of these 3 diseases using ddPCR in order to ensure that the mutation can be detected in patient samples
3. Analyze the correlation between ctDNA and serum monoclonal IgM (today's monitoring of the disease) in Waldenstrom patients
4. Estimate how much serum and how much cfDNA are necessary to detect the mutation if there is an active disease or remission period
5. Compare serum vs plasma samples as a source for ctDNA, evaluate whether there are significative differences in the results obtained in both blood fractions.

For this master thesis the focused was on the first aims 1 to 4.

3. Material and Methods

3.1. Clinical samples

The study was approved by the Regional Committees for Medical and Health Research Ethics (REK), REK number 2016/1156, and a written informed consent was acquired from all patients.

A total of 43 serum and 23 plasma samples from 13 patient samples were provided by the hematology department, St Olav's Hospital and Biobank1. Healthy donors' samples were provided from the blood bank (St Olav's Hospital).

An overview of the patient samples used and some clinical info of each patient is shown in Table *1*. The clinical information of each patient was provided after the experimental analysis was performed.

Patient	Disease	Timepoints	Sex
1	WM	1	-
2	WM	1	-
3	WM	1	M
4	WM	1	-
5	IgM-MGUS	1	F
6	WM	1	M
7	WM	1	-
8	WM	1	M
9	WM	19	M
10	HCL	3	F
11	HCL	1	-
12	APL	7	F
13	APL	5	M
Total	-	**43**	-

Table 1 Overview of the patient samples analyzed

3.2. Blood sample processing

Patients and healthy donors' samples were processed within 2 hours after blood collection. Serum samples were collected in Vacuette Tube 9mL, Z serum clot activator. The process of serum is shown in Figure 12. First, serum samples were left to coagulate at least 30 minutes. Afterwards, samples were centrifuge at 2200g for 10 minutes. Then the supernatant was transferred again into a 2mL cryotube and was storage at -80.

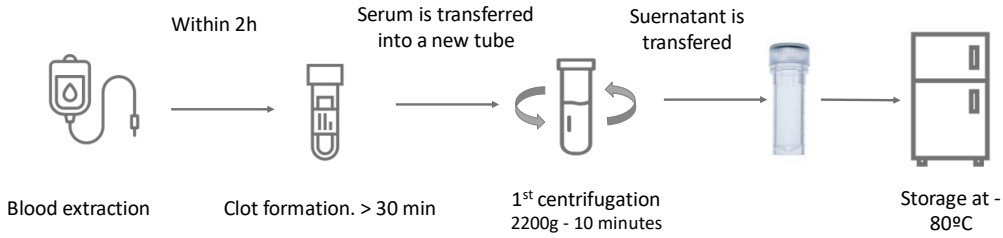

Figure 12 Blood sample processing

On average 2,9 mL/sample of serum was received from healthy donors (range from 1,8mL to 3,64mL) and 1,8 mL/sample of serum from patients (range from 0,76mL to 3,2mL) to use in this study.

3.3. Circulating free nucleic acids isolation

First, serum samples were thawed and centrifuged at 4000g for 10 minutes. cfDNA was extracted from serum samples using QIAamp Circulating Nucleic Acid Kit (Qiagen, Germany). The extraction was done according to the manufacturer's protocol using QIAamp Mini columns on a vacuum manifold QIAvac 24 Plus.

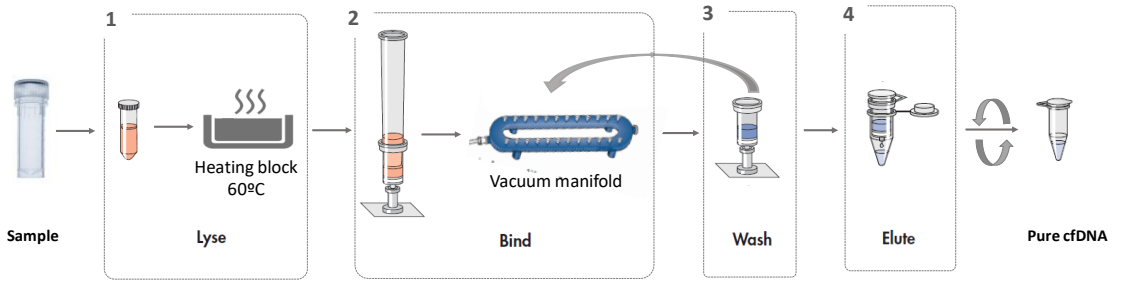

Figure 13. Cell free DNA extraction process. Adapted from QIAamp Circulating Nucleic Acid Handbook

QIAamp Circulating Nucleic Acid procedure involve 4 steps, lyse, bind and elute

1) In the first step, samples are lysed under high temperature conditions in the presence of proteinase K and buffer ACL in order to allow circulating nucleic acids to be release from bound proteins or vesicles.
2) The second step involve the binding of the nucleic acids to the membrane of the column. The nucleic acids are adsorbed in the membrane as the lysate is drawn through by vacuum pressure.
3) After the lysate have passed through the column, three washing steps are carried out using wash buffers and ethanol in order to remove the remaining contaminants, meanwhile the nucleic acids remain attached to the membrane.

4) In the last step, nucleic acids are eluted from the membrane by centrifugation, using 50µL elution buffer.

Once the pure nucleic acids were obtained the concentration was measured and the eluate was frozen at -20ºC until ddPCR experiments were performed

cfRNA extraction

cfRNA was extraction was done with the same kit as for cfDNA, QIAamp Circulating Nucleic Acid Kit (Qiagen, Germany) but with some modifications. Protein kinase incubation time was extended to 1h instead of 30 min and RNA carrier was not used.

Concentration measurement

Right after the extraction of cfNA (circulating nucleic acids), the concentration in the eluate was measured using NanoDrop™ 1000 Spectrophotometer (Thermo Fisher Scientific). Before ddPCR experiments, a more accurate measurement of the DNA concentration was carried out with Qubit® dsDNA HS (High Sensitivity) Assay Kits. This kit is designed to provide an accurate quantification of samples with DNA concentration between 0.2-100 ng/µL (69).

The average concentration of cfDNA obtained from healthy donor's was 34 ng/mL of serum (range from 24 ng/mL to 51 ng/mL), and 38 ng/mL of serum (range from 19 ng/mL to 99 ng/mL) from patient samples.

Bioanalyzer

The principle of the bioanalyzer is to perform highly accurate DNA electrophoresis, measuring precise size and concentration of all DNA fragments, both small and large, using small volumes. After cfDNA extraction, some of the samples were select for its analysis in the bioanalyzer in order to check that the cfNA were isolated successfully. Thus, 10 samples were analysed in an Agilent chip. Results in Figure 5S (appendix).

3.4. Digital Droplet PCR

Workflow

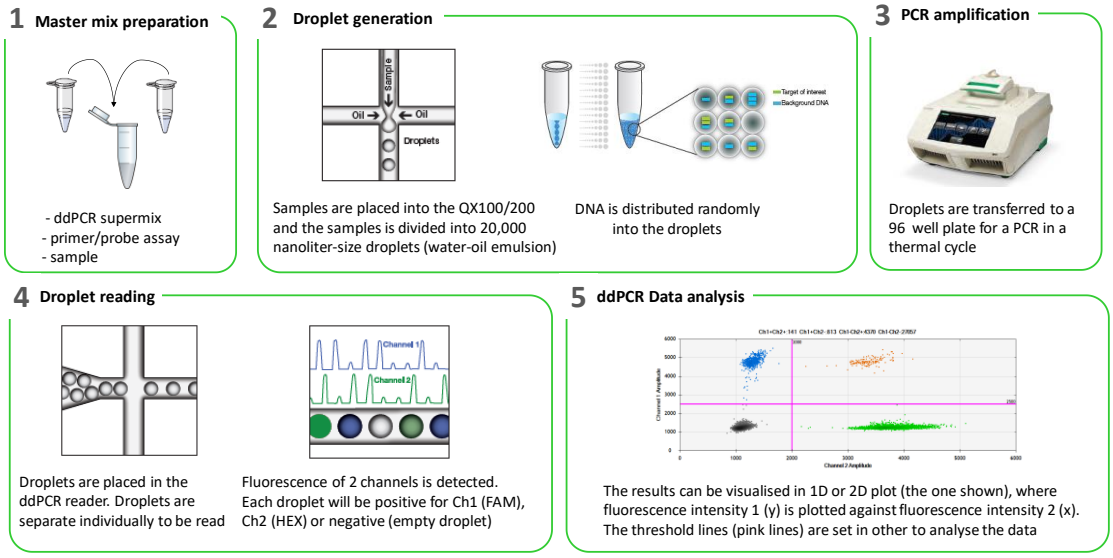

Figure 14 ddPCR Workflow. Pictures from step 2, 3 and 4 are taken from Digital Droplet PC Applications Guide (Bio-Rad) (61)

Figure 14 shows the workflow of the experiment with ddPCR, from sample preparation until data analysis. 1) Master mix preparation: ddPCR supermix for probes (No dUTP) is mixed together with primer and probes of the assay, the assays contain 2 probes, FAM (Carboxyfluorescein) for the mutated molecules and HEX for the wild types (WT). 2) Droplet generation: the droplet generator creates the droplets as a water-oil emulsion, in each sample 20,000 droplets are generated; 3) PCR amplification; 4) Droplet reading, each droplet is individually separated and the fluorescence of each probe is detected. The reader counts the number of droplets positive for each probe 5) Data analysis: QuantaSoft™ Software estimates the concentration of copies in the starting material based on positive droplets following Poisson distribution (61).

When generating the droplets, the DNA molecules in the sample are randomly distributed into the 20,000 droplets. Thus, each of the droplets can contain 0 molecules, 1 molecule, 2 molecules or more. As a result, 4 clusters can be obtained Figure 15:

- FAM negative, HEX negative (empty droplets) - Ch1-Ch2-
- FAM positive, HEX negative (droplet with one or more mutated molecules). Ch1+Ch2-

- FAM negative, HEX positive (droplet with one or more WT molecules) Ch1-Ch2+
- FAM positive, HEX positive (droplet with two or more molecules, both mutated and wildtype) - Ch1+Ch2+

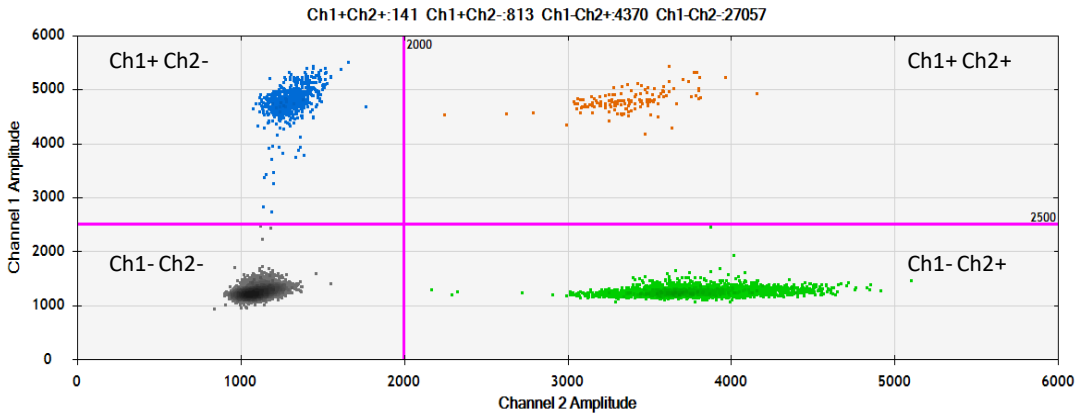

Figure 15. 2D ddPCR plot of one of the results. Pink lines show the threshold that are manually adjusted, meaning that all the dots under the lines will be considered negative for the channel/probe that is being analysed. Grey dots, are negative for both probes, thus, are droplets that do not contain any molecule. Green dots are positive for the WT probe (HEX) - Ch2, and negative for Ch1 (FAM) meaning that those droplets contain only WT molecules. Blue dots are positive for the mutated probe (FAM) – Ch1 and negative for HEX, Ch2, meaning that those droplets contain just mutated molecules. The last cluster, orange dots, are positive for both probes/channels, meaning that in that droplets more than one molecule is present, one is mutated (FAM fluoresce) and the other is WT (HEX fluoresce)

3.4.1. Assays – primer / probes

Commercial pre-validated primer/probe assays were used for the mutation Myd88 L265P and BRAF V600E (PrimePCR ddPCR Mutation Assays, Bio-Rad). Primer and probe sequence of these assays is not available. In the case of PML-RARA, the primer and probes were designed and ordered from the manufacturer, as described below.

The assays, mutated and a wild type assay, consist of forward and reverse PCR primers and a dual labeled fluorescent probe, FAM fluorochrome for the mutation assay and HEX fluorochrome for the wild type assay. Figure 16 is a graphic representation of how the probes in the assays works.

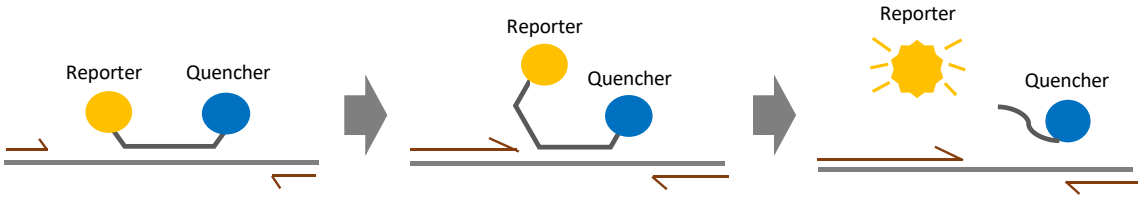

Figure 16 Dual fluoresce probe used in the assays. In the annealing step, the probe binds to its target, when the extension step takes place the probe is displaced and he reporter fluorochrome is cleavage and emits fluorescence. The function of the quencher is to inhibit the fluoresce when the reporter is near to it. [Image adapted from Droplet Digital PCR Applications Guide, Bio – Rad].

PML-RARA assay primer/probe design

Wild type assay

The forward and reverse primer and the probe HEX for the WT assay were located in exon 2 of PML gene (NM_033238.3) as it is shown in Figure 17. In order to simplify the representation and show both primers (forward and reverse) and the probe in the same mRNA sequence, the complement sequence of the reverse (R) primer and probe has been represented.

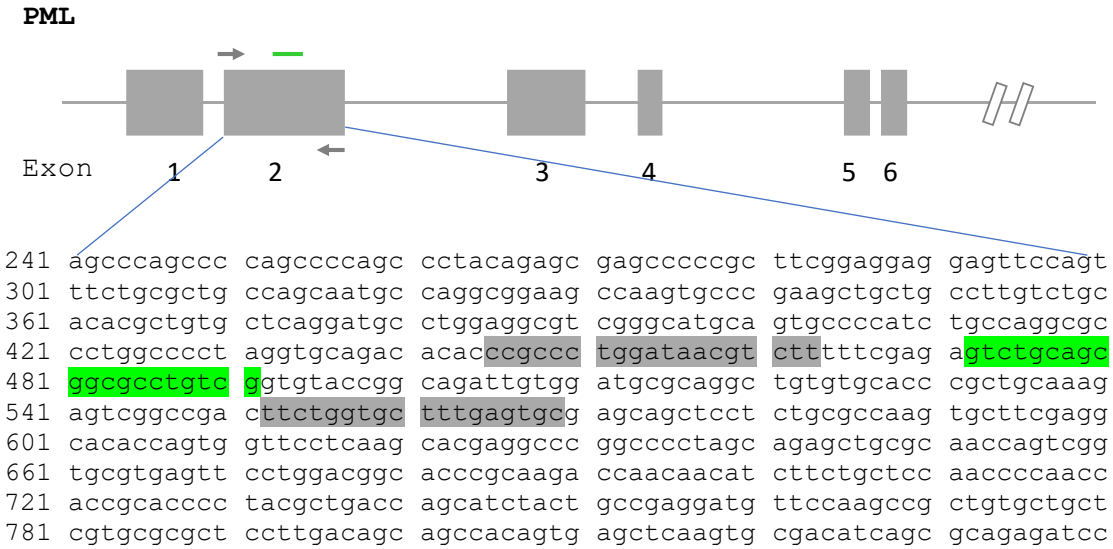

Figure 17 Sequence of exon 2 PML gene. Primer/probe location. Exon 2: 440…472; Grey arrows in the gene (scheme) and grey highlighted sequence show the revers and forward primers. Green line in the gene (scheme) and green highlighted sequence show the probe HEX

Forward primer: ccgccctggataacgtcttt
Reverse primer: gcactcaaagcaccagaagt (complementary: acttctggtgctttgagtgc)
Probe: cgacaggcgccgctgcagac (complementary: gtctgcagcggcgcctgtcg)

Mutated assay

The primers and probes used for the translocation were from a previous publication (40). For both fusion transcripts the reverse primer and probe are located in exon 3 of RARA gene (NM_000964.4) as it is shown in Figure 18. In the case of Bcr1_2 transcript the primer is located in exon 6 (NM_033238.3). In the case of Bcr3 a new primer was added to the assay

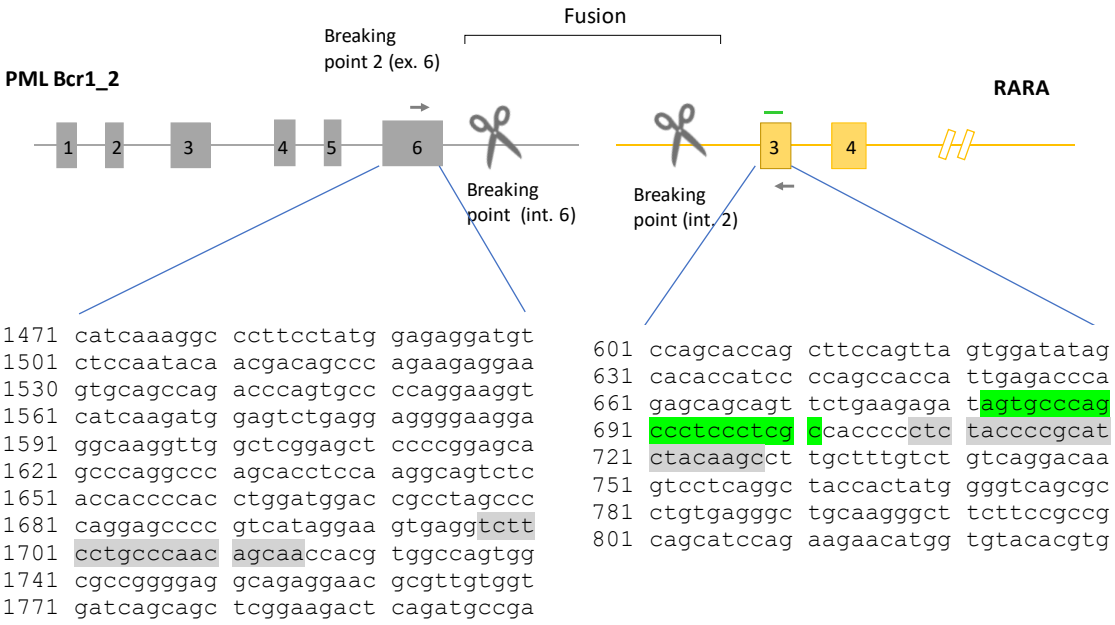

Figure 18 Sequence of exon 6 PML gene and exon 3 RARA gene. Primers/probe location. Exon 6 PML: 1496...1754; Exon 3 RARA: 648...796; Grey arrows in the gene (scheme) and grey highlighted sequence show the revers and forward primers. Green line in RARA gene (scheme) and green highlighted sequence show the probe FAM

Forward primer: tcttcctgcccaacagcaa

Reverse primer: gcttgtagatgcggggtagag (complementary: ctctaccccgcatctacaagc)

Probe: agtgcccagccctccctcgc (complementary: gcgagggagggctgggcact)

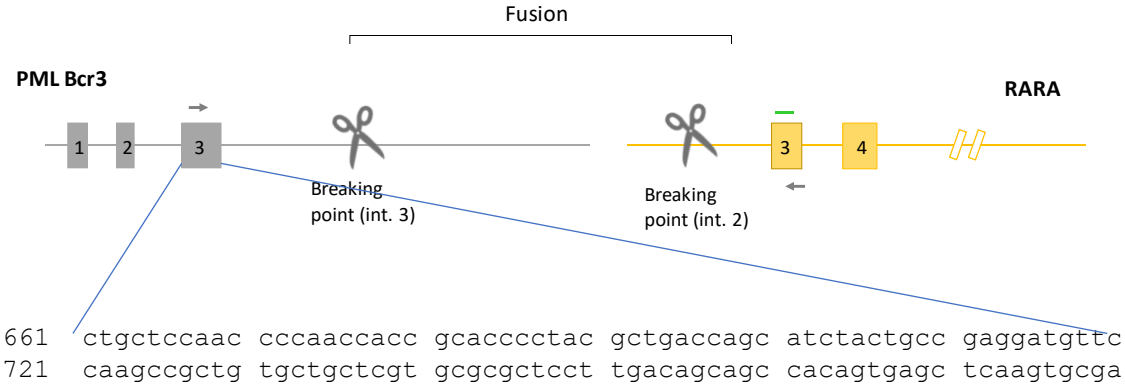

```
781  catcagcgca gagatccagc agcgacagga ggagctggac gccatgacgc aggcgctgca
841  ggagcaggat agtgcctttg gcgcggttca cgcgcagatg cacgcggccg tcggccagct
901  gggccgcgcg cgtgccgaga ccgaggagct gatccgcgag cgcgtgcgcc aggtggtagc
961  tcacgtgcgg gctcaggagc gcgagctgct ggaggctgtg gacgcgcggt accagcgcga
1021 ctacgaggag atggccagtc ggctgggccg cctggatgct gtgctgcagc gcatccgcac
1081 gggcagcgcg ctggtgcaga ggatgaagtg ctacgcctcg gaccaggagg tgctggacat
1141 gcacggtttc ctgcgccagg cgctctgccg cctgcgccag gaggagcccc agagcctgca
1201 agctgccgtg cgcaccgatg gcttcgacga gttcaaggtg cgcctgcagg acctcagctc
1261 ttgcatcacc caggggaaag atgcagctgt atccaagaaa gccagcccag aggctgccag
```

Figure 19 Sequence of exon 3 PML gene. Primers/probe location. Exon 3 PML: 700..1280; Grey arrows in the gene (scheme) and grey highlighted sequence show the forward primer.

Forward primer: ccgatggcttcgacgagtt

Reverse primer: same as in assay for Bcr1_2

Probe: same as in assay for Bcr1_2

Apart of the primers already mentioned, another primer was design in RARA gene at the end of the exon 2, shown in Figure 20.

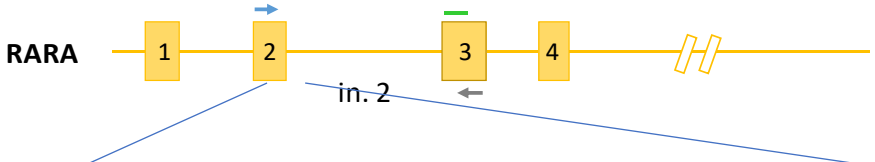


```
61   ttctcctggg aaccccatcg gccccctgcc agcacacacc tgagcagcat cacaggacat
121  ggcccccтca gccacctagc tggggcccat ctaggagtgg catcttttтt ggtgccctga
181  aggccagctc tggaccttcc caggaaaagt gccagctcac agaactgctt gaccaaagga
241  ccggctcttg agacatcccc caacccacct ggcccccagc tagggtgggg gctccaggag
301  actgagatta gcctgccctc tttggacagc agctccagga cagggcgggt gggctgacca
361  cccaaacccc atctgggccc aggccccatg ccccgaggag gggtggtctg aagcccacca
421  gagccccctg ccagactgtc tgcctccctt ctgactgtgg ccgcttggca tggccagcaa
481  cagcagctcc tgcccgacac ctgggggcgg gcacctcaat gggtacccgg tgcctcccta
541  cgccttcttc ttccccccta tgctgggtgg actctccccg ccaggcgctc tgaccactct
601  ccagcaccag cttccagtta gtggatatag cacaccatcc ccagccacca ttgagaccca
```

Figure 20 RARA gene, exon 2. New primer. Exon 2: 108…647. In blue it is shown the new reverse primer designed. This primer, together with the reverse primer and probe in exon 3 (mutant ddPCR assay) will give product just in RNA transcripts (where introns have been already removed).

Forward primer: cactctccagcaccagcttc

Reverse primer: same as in assay for Bcr1_2

Probe: same as in assay for Bcr1_2

A brief summary of the mutations and the assays used is shown in Table 2

Malignancy	Waldenstrom Macroglobulinemia	Hairy Cell Leukemia	Acute Promyelocytic Leukemia
Gene	Myd88	BRAF	PML / RARA
Cytogenetic Location	3p22.2; chr3:38179969-38184512	7q34; chr7:140433813-140624564	15q24.1; chr15:74,287,014-74,340,155 / 17q21.2; chr17:38,465,423-38,513,895
Type of mutation	Point mutation / Missense	Point mutation	Translocation
mRNA change (nt)*	c. 978 T>C	c. 1799 T>A	Bcr1 (int. 6) / Bcr2 (ex. 6) / Bcr3 (in. 3)
Protein change (aa)	p. L265P	p. V600E	-.
Positive control	gBlock	HT29	gBlock
Unique assay ID mut/WT	dHsaIS2506944, dHsaIS2506945	dHSAcp2000027, dHSAcp2000028	Own design
Forward primer	Not available	Not available	ccgccctggataacgtcttt (WT) tcttcctgcccaacagcaa (Bcr1_2) ccgatggcttcgacgagtt (Bcr3) cactctccagcaccagcttc (PML ex 2)
Reverse primer	Not available	Not available	gcactcaaagcaccagaagt (WT) gcttgtagatgcggggtagag (Bcr1_2 and Bcr3)
Length amplicon (nt)	65	91	-
WT probe (HEX)	Not available	Not available	cgacaggcgccgctgcagac
Mutant probe (FAM)	Not available	Not available	agtgcccagccctccctcgc

Table 2. Digital Droplet PCR assay information. * different transcripts for PML-RARA

3.4.2 Controls

All ddPCR experiments require internal controls in order to ensure that the results are reliable and trustful. In all the experiments, 3 µL of the controls were used for the ddPCR reaction (the concentration is specified in each control).

- **Negative control (NC):** genomic DNA from peripheral blood from a healthy donor at a concentration of 4ng/µL, 1,212 copies per µL. The same sample was used in all NC ensuring reliability between different experiments. We expected the negative control to be positive for the probe HEX that detect the wild type (WT) sequence of the gene. NC is important for the estimation of the false positive rate of the assay. It also shows that the assays are well design and there are not non-specific bindings and contamination
- **Positive control (PC):** This control is different depending on the assay.
  - BRAF assay: HT-29. Cell line from ATCC®. Colorrectal adenocarcinoma. (Homo Sapiens). It has a heterozygous BRAF V600E mutation. The experiments showed that 25% of the molecules have the mutation. The concentration used was 4ng/µL, 1.212 copies per µL
  - Myd88: a gBlock sequence with the mutation was design, Figure 6S Appendix A concentration of 1.000 copies per µL was used

- PML-RARA: 2 gene blocks were used. Bcr1_2 gene block and Bcr3 gene block. Their sequence, as well as primer/probe in the sequence is shown in figure 7S Appendix. A concentration of 1.000 copies per µL was used

The PC is expected to be positive for FAM probe (mutated). It tests the assay performance and also shows the mutated cluster.

- **Non-template control (NTC):** H_20 is used as non-template control. This control has the purpose of detecting environmental or cross-contamination. When this is negative (no signal detected in the well) it indicates a clean technique and good laboratory practices

3.4.3. Protocol

QX200™ Droplet Digital PCR (Bio-Rad Laboratories GmbH, Munich, Germany) was the platform used for this research. the data analysis was performed using the QuantaSoft™ Software. All experiments and sample handling were done under good laboratory practices following the hospital routines.

The master mix for the PCR had a final volume of 20 µL containing:

- 10 µL of the ddPCR supermix for probes (No dUTP)
- 1 µL of each primer/probe mix (1 µL WT primer/probe - HEX and 1 µL mutated primer/probe – FAM). The concentration of the primer/probe is already established by the manufacturer being 450nM and 250nM respectively
- 6 µL of sample (patient and healthy donors), out of the total of 50 µL eluate. Triplicates were made for each sample. For the controls and limit of detection experiments, 3 µL of each are used mix together with 3 µL of H_20 adding a total volume of sample of 6 µL (controls concentrations are shown in the "controls" section).
- H_20 is used to reach the 20 µL reaction.

Once the PCR mix is prepared, the 20 µL mix are transferred into a cartridge together with 70 µL of oil Figure 21.

Figure 21. ddPCR cartridge for droplet generation. The cartridge with 20uL of PCR mix and 70uL of oil goes into the droplet generator to generate the droplets.

Once the droplets are generated, 40uL are transfer to a 96 well plate for PCR amplification. Thermocycling conditions were 95ºC for 10 minutes, followed by 40 cycles at 94°C for 30 seconds, annealing temperature at 55ºC for 1 minute and 10 minutes stabilizing step at 98°C.

The same volumes, concentration and thermal conditions are used for the 3 assays.

Afterwards, droplets were read using the QX200 Droplet Reader and data was analyzed using the QuantaSoft™ Software v.7.0.1. Wells with less than 9000 accepted droplets were not considered for the analysis.

The master mix and droplet generation were performed in a pre-PCR area to prevent contamination from DNA in the PCR area.

3.4.4. Limit of Detection and False Positive Rate

Limit of Detection (LoD) is defined as the minimum concentration of the mutation that can be reliable differentiated from a Wild Type background (negative control) and its usually given as a percentage (0,01%). 1 mutated copy in 10.000 wild type molecules.

LoD is performed to evaluate the specificity of the assay, that is the ability to detect a mutated copy out of several wild type molecules. A low LoD for an assay indicates a highly of sensitivity, since is able to detect a very low copy number in a highly concentrated wild type background. When testing patient samples, as long as the results are within the limit of detection range of the assay, they can be considered reliable.

The LoD is obtained doing serial dilutions of a mutated molecule (the positive control used for the assay) in a constant WT background (mutant + genomic DNA). Figure 22 shows an example of the linear regression graph obtained.

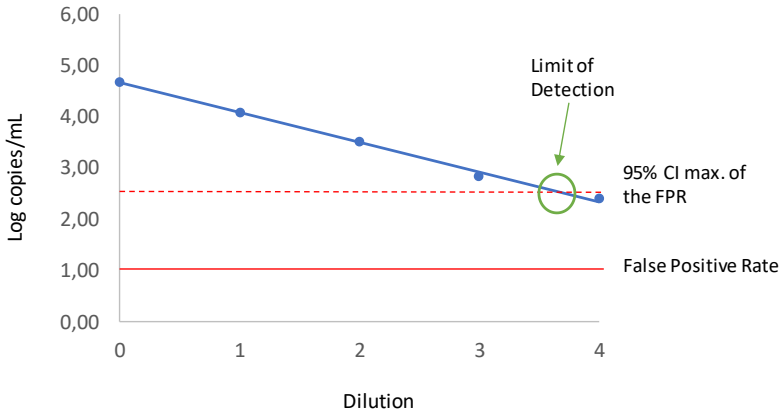

Figure 22. Example of Limit of Detection. Linear regression. The 5 dots show the serial dilutions of a mutated molecule in a constant background of WT molecules. Red line shows the false positive rate of the assay. The green circle shows the Limit of detection of this assay.

The Limit of Detection (LoD), was determined based on the the upper value of the upper 95% confidence interval of the false positive rate. The lowest error bar of the last dilution does not have to overlap with the upper CI error bar of the negative control, WT, if it overlaps, the previous dilution will be considered for the LoD.

The False Positive Rate (FPR), is the copies that are measured as positive for the mutation when they should be negative, due to errors in the technology or unspecific binding of the primers. It is determined with the WT and none template controls and it is defined as the fractional abundance for the mutant molecule at the upper 95% Poisson CI for the WT control. Fractional abundance is explained as the mutated fraction divided by the total number of molecules.A low false positive rate indicates a highly specific assay Figure 22.

Since three different assays (one per mutation/disease) were used, a LoD test was done for each assay. In the case of PML-RARA assay, 2 different fusion transcripts were analyzed, and thus, two LoD test were done, one for each transcript Bcr1_2 and Bcr3.

The dilutions made for the LoD were 4-fold serial dilutions of each mutated target in a constant background of genomic DNA. A starting concentration of 1000 copies/ µL of each mutated target was used, the resulting copy number tested was 1000 (1:1) – 250 (1:4) – 63 (1:16)– 16 (1:64) – 4 (1:256) – 1 (1:1024) mutated copy in a background of 1212 WT copies. 3 µL of each of the dilutions were mixed with 3 µL genomic DNA (constant WT background), at a concentration of 4 ng/µL (total of 6uL of sample).

Positive and negative controls were included in all LoD experiments, (same volumes and concentration as in the rest of the experiments were used (see 3.4.3 Controls and 3.4.3 Protocol).

3.3.5. Data analysis and thresholds

The analysis of the data was done with QuantaSoft™ Software version 1.7 and Microsoft Excel 2010. Absolute quantification (ABS) was chosen for all experiments. Once the droplet reader interrogates every single droplet for both probes (FAM and HEX), QuantaSoft™ Software set up automatic thresholds and determines the concentration of mutant and wild type molecules based on Poisson distribution. However, for the correct designation of the droplet population the thresholds must be adjusted manually in the 2D plot based on the controls (PC, NC and NCT). This is shown in Figure 23. Once the thresholds have been adjusted QuantaSoft™ Software shows the correct concentration reported as copies/µL of the final 1x ddPCR reaction.

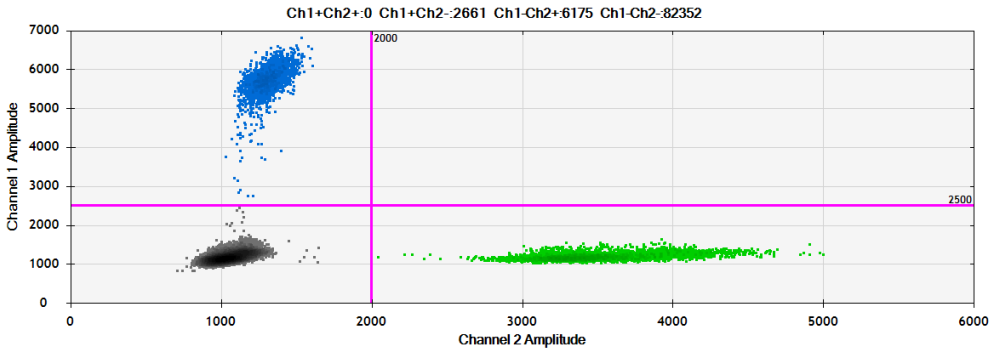

Figure 23 2D amplitude plot. Set up of thresholds. In the plot, PC, NC and NTC controls are shown. A good separation between the different droplet clusters should be achieved to ensure the correct designation of the droplets as negative (grey) or positive (blue or green). The threshold is adjusted based on the clusters given by the controls. Threshold: Ch1 2500; Ch2 3000.

3.5. Workflow

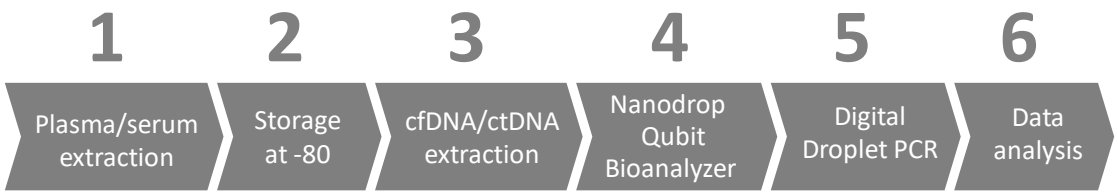

Figure 24. Work flow of the whole process. Process since we received the blood sample until we obtained the results.

This master thesis began in step 3. After serum samples were thawed, the isolation of cell free DNA or circulating tumor DNA was carried out for each sample. Every sample was eluted in 50 µL of elution buffer. Then, the concentration of the cfDNA in the eluate was measured using nanodrop/Qubit. Afterwards, the ddPCR experiment was performed. Three replicas were done using 6 µL of the eluate in each one. Thus, a total of 18 µL out of the 50 µL of eluate was analysed for each patient. Results from the ddPCR were normalized taking into account the starting material volume (mL of serum received from each patient) by dividing the number of mutated copies found in the 50 µL eluate by the starting volume.

4. Results

This master thesis includes the study of 13 patients with three different hematological malignances, Waldenstrom Disease, Hairy Cell Leukemia, Acute Promyelocytic Leukemia in addition to one patient diagnosed with IgM – MGUS (Table 1). These diseases are chosen as they all have one specific mutation, or translocation (APL), that are present in the majority of the patients (90-100%).

Digital Droplet PCR analysis

The results are shown in three different sections according to the three malignances included in the study.

Prior to the analysis of the patient samples, it is first necessary to determine the False Positive Rate (FPR) and Limit of Detection (LoD) for each assay for the accurate detection and quantification of the target molecule.

4.1. Waldenstrom Macroglobulinemia

Limit of Detection and False positive rate

For the study of WM, the mutation L265P in the gen Myd88 was targeted. First a 1:10 serial dilution of mutated DNA fragments was tested (figure 8S, Appendix), but was later changed to 1:4 serial dilutions, since the critical concentration was found to be in the area between 10 to 1 copy. The positive copies used were the gene blocks showed in Figure 1S in Appendix (see section 3.4.2. Controls). Table 3 lists the theoretical and acquired number of copies in the LoD experiment (per PCR reaction).

	Expected results		Experimental results		
Dilutions and controls	**Mutated copies***	**WT copies***	**Mutated copies***	**WT copies***	**Fractional abundance (%)**
1:1	3000	3636	3780	3100	55,6
1:4	750	3636	-	-	-
1:16	188	3636	182	3212	5,4
1:64	47	3636	40,2	2778	1,41
1:256	12	3636	11,2	3128	0,36
1:1024	3	3636	1,6	3216	0,05
NC (wt)	0	3636	0	3780	0
PC	3000	0	3436	-	100
NTC	0	0	0	0	0

Table 3 Myd88 L265P LoD results. Theoretical and acquired number of copies across the different dilutions. *Copies in the 20µL PCR reaction. Dilution 1:4 was skipped since it was already tested in the previous 1:10 LoD. NC: negative control; PC: positive control; NTC: non template control.

The wild type background remains stable, and the mutated copies decrease according to the theoretical dilution curve (Figure 25), as confirmed by a R-squared value of 0,99 (Figure 26).

a)

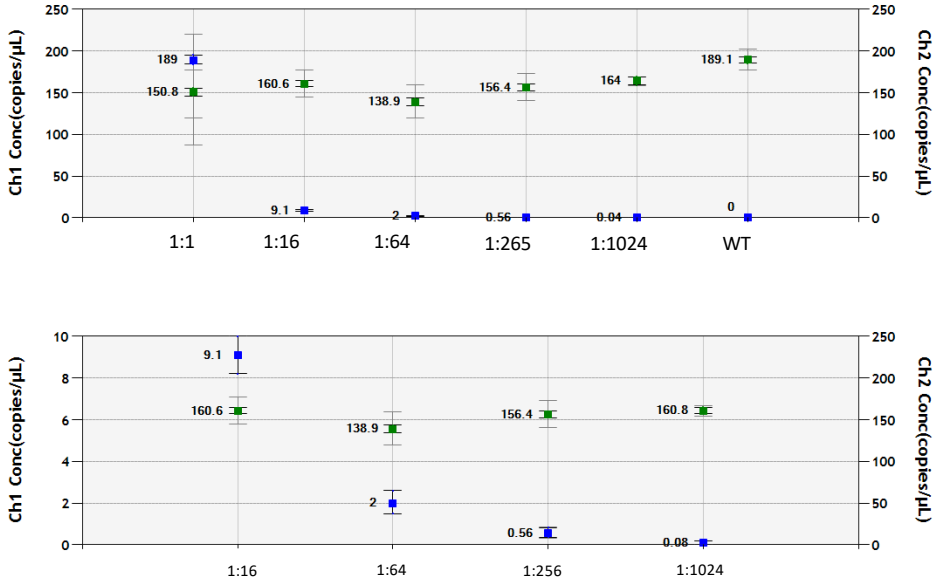

b)

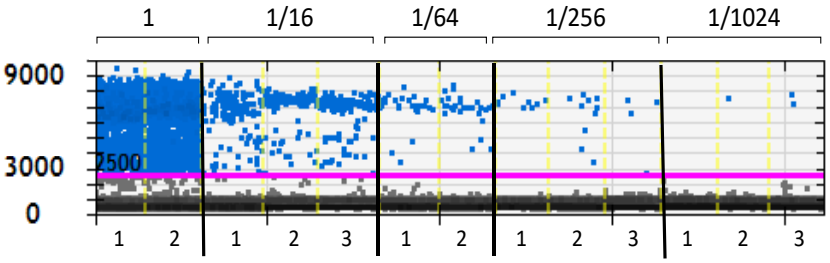

Figure 25. 2D and 1D amplitude plot. Dilution test LoD. a) Concentrations are given as copies per 1uL PCR reaction (20uL PCR reaction in total). Green square - Wild Type concentration (HEX) remains constant. Blue square - mutant concentration, decrease according to the serial dilutions. Negative controls (WT) and NTC shows no false positive droplets. **b)** Blue dots are positive droplets for the mutation (FAM). 2 or 3 replicas of each dilution are analysed.

The FPR was acquired according to the three negative controls (WT) of the experiment. It was found to be 0%, the upper 95% CI was 1,18 copies per PCR reaction. Thus, combining the dilution curve, the false positive rate and its 95% CI the limit of detection for this assay is set at an allele frequency of 0.05% meaning that 5 copies can be reliable called true positive in a background of 10.000 WT molecules. When applied to patient samples, those with a mutation rate above the LoD 0.05% were considered true positive.

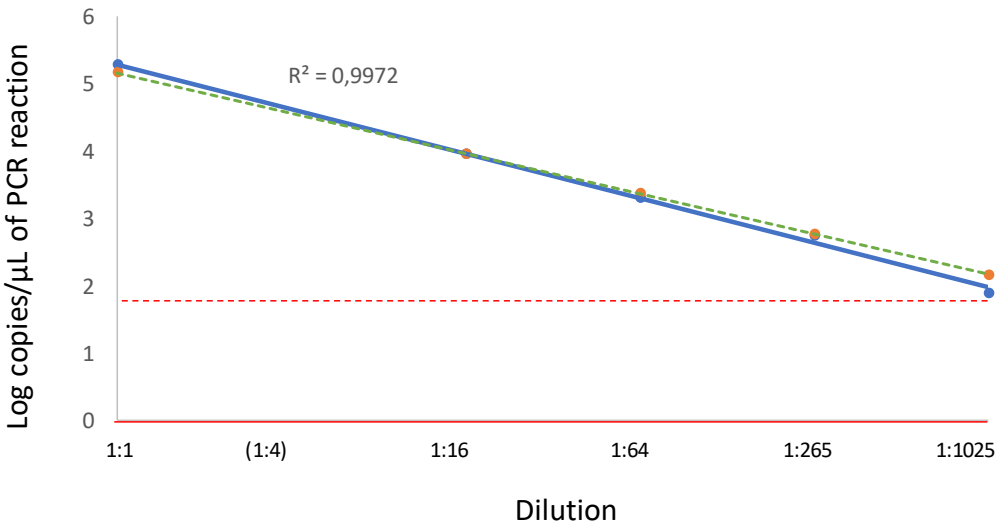

Figure 26 Limit of Detection for Myd88 L265P assay (Waldenstrom Macroglobulinemia). The graphic shows $\log_{10}$ of the mutated concentration (copy number per µL of ddPCR reaction) plotted against the corresponding dilutions. Blue line – experimental results. Green dotted line – expected results. The curve is transformed into a linear regression, being R^2= 0,99. The red line shows the false positive rate based on 8 healthy donors. The dotted red line shows the Poisson 95% CI of the FPR. The LoD, was determined based on the upper value of the 95% confidence interval of the false positive rate

Patients samples

Eight patients diagnosed with Waldenstrom Macroglobulinemia in addition to one IgM MGUS patient were tested for Myd88 L265P mutation. One sample per patient was analyzed except for patient #6 where we had 19 different timepoints taken during a period of 9 years (Table 1). In all the patients 3 replicas of 6µL of sample were performed and showed as a merge, Thus, a total of 18µL of eluate per patient was analyzed.

First, a mix of cfDNA from 9 healthy donors (HD) in 8 replicates was analyzed in order to test if the mutation Myd88 L265P can be found in HD or it is specific for patients, Figure 27. The average concentration of the 9 HD samples was 1,6 ng/µL (range of 1,4 ng/µL to 1,8 ng/µL in the eluate). The resulting pool had a concentration of 1,36ng/µL.

One of these replicates showed one positive droplet for the mutation. This droplet is located in the cluster Ch1+Ch2+ and it is near to the threshold, previously established at 2500/2000 amplitude (as explained in section 3.3.5).

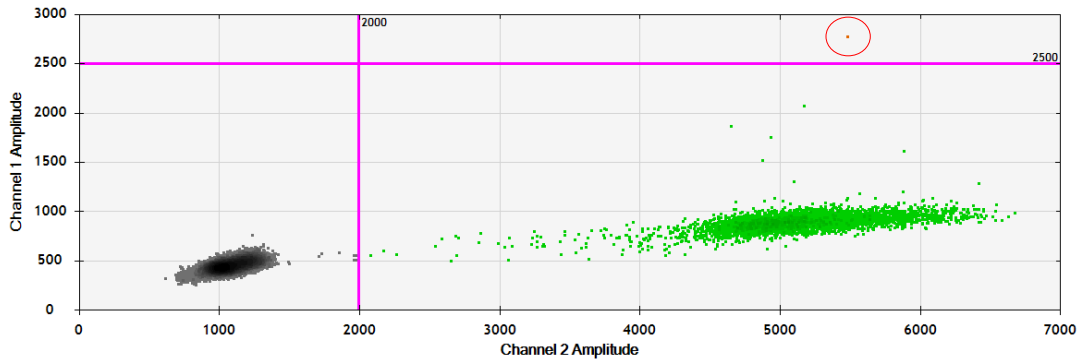

Figure 27 2D amplitude ddPCR plot for healthy donor merge. Ch1+Ch2+: 1; Ch1+Ch2- : 0; Ch1-Ch2+: 5357; Ch1-Ch2-: 85101. The red circle shows the positive droplet found for both, FAM and HEX probe

Out of the 9 patients tested for the mutation Myd88 L265P, 4 of them were clearly positive with an allele frequency significantly above the LoD of the assay (> 0.05%). 2 of the patients were negative for the mutation, having 0 mutated copies in the sample tested. The remaining 3 patients were positive for mutation but with an allele frequency quite near to the LoD. A summary of the main findings of these patients is shown in Table 4.

Patient	cfDNA (ng/mL serum)	Mutated copies in PCR reaction	Mutated copies / mL serum	WT copies in PCR reaction	Fractional abundance (%)	M component (G/L)	Overall result
1	36	132	183	3882	3,3	6,7	Positive
2	52	2032	2090	11260	15	25,4	Positive
3	50	336	363	9660	3,7	6,8	Positive
4	19	1,8	2,1	2480	0,07	7,5	Uncertainty
5	34	5,8	8	4340	0,13	2,5	Uncertainty
6	34	2,2	4,4	4300	0,05	1,00	Uncertainty
7	31	0	0	3224	0	0,1	Negative
8	20	0	0	2546	0	0,7	Negative

Table 4 Main ddPCR results and clinical information of each patient. 3 replicates containing 6µL of sample were tested for each patient; ddPCR results are given for the total of 18 µL sample tested.

The results of each patient will further be discussed presented with clinical data and comparison with IgM curves. To verify if the results are consistent, the patient's IgM curve was provided (Appendix figure 9S)

Patient 1

The ddPCR results (Table 4) showed positive droplets for the mutation clustered in the Ch1+Ch2- and Ch1+Ch2+ region at an amplitude of 7000 of the FAM probe (red circle Figure 28). Also, positive droplets for the WT probe were detected. According with Poisson distribution this corresponded to a concentration of 132 mutated and 3882 wild type molecules in the PCR reaction. The fractional abundance was 3,3%, clearly above the LoD test, and therefore defined as a true positive sample.

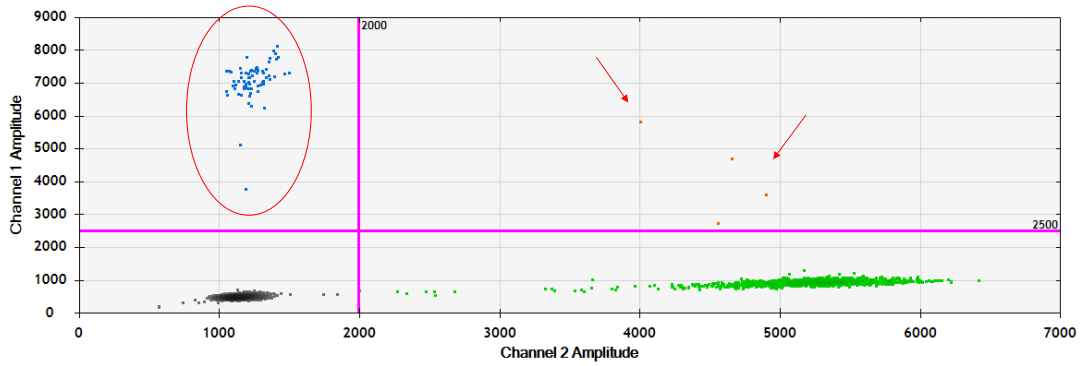

Figure 28. 2D amplitude ddPCR plot for patient 1. Ch1+Ch2+: 4; Ch1+Ch2- : 71; Ch1-Ch2+: 2132; Ch1-Ch2-: 38008. Merge of 3 replicas of the patient 1 (6 µL each). A total of 18µL of the 50µL eluate was tested. Blue and orange dots show positive droplets for the mutation Mydd88 L265P. Green dots shows positive droplets for the WT molecule

According to the clinical data, this patient, diagnosed with Waldenstrom Macroglobulinemia, had not received treatments during the last 2 years. The IgM-value at time of sample was 6,7G/l and it showed an increasing tendency. The M component curve is shown in figure 9S (supplementary material).

The results from the ddPCR are then in line with the clinical data of the patient.

Patient 2

The results from the ddPCR showed positive droplets for the mutation, clustered in Ch1+Ch2- and Ch1+Ch+ region (red circle and red line Figure 29) and positive droplets

for the WT probe. This corresponded to a concentration of 2032 mutated and 11260 WT molecules in the PCR reaction, resulting in a fractional abundance of 15,3% (Table 4). This patient was a clear positive patient for the mutation Myd88 L265P.

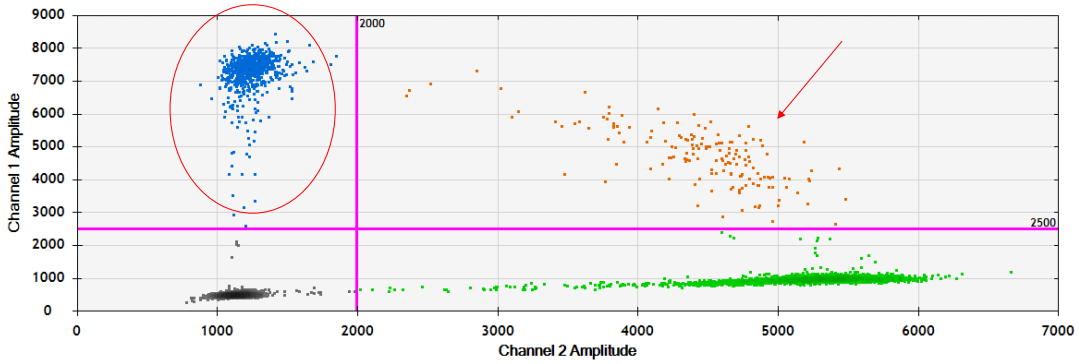

Figure 29 2D amplitude ddPCR plot for patient 2. Ch1+Ch2+: 158; Ch1+Ch2- : 816; Ch1-Ch2+: 4914; Ch1-Ch2-: 28627. Merge of 3 replicas of the patient 2 (6 µL each). A total of 18µL of the 50µL eluate was tested. Blue and orange dots show positive droplets for the mutation Mydd88 L265P. Green dots shows positive droplets for the WT molecule.

The clinical data for this patient diagnosed with Waldenstrom Macroglobulinemia, showed that at the time of the sample date October 2018 the patient was not being treated (since June 2018). At the time of the sample the patient had an active disease with and increasing M component curve, the IgM value was 25.4 G/L. (figure 9S supplementary material).

Thus, the positive result from ddPCR had a good correlation with the clinical data showing an active disease.

Patient 3

For patient 3, digital droplet PCR results (Table 4) showed positive droplets for the mutated probe in the regions Ch1+Ch2- and Ch1+Ch+ (red circle and line in Figure 30) as well as for the wild type probe. According to Poisson distribution, this corresponded to a concentration of 336 mutated and 9660 wild type molecules in the ddPCR reaction. The mutated fractional abundance of this patient is 3,7%, above the LoD. Thus, results from ddPCR shows that the patient is positive for the mutation.

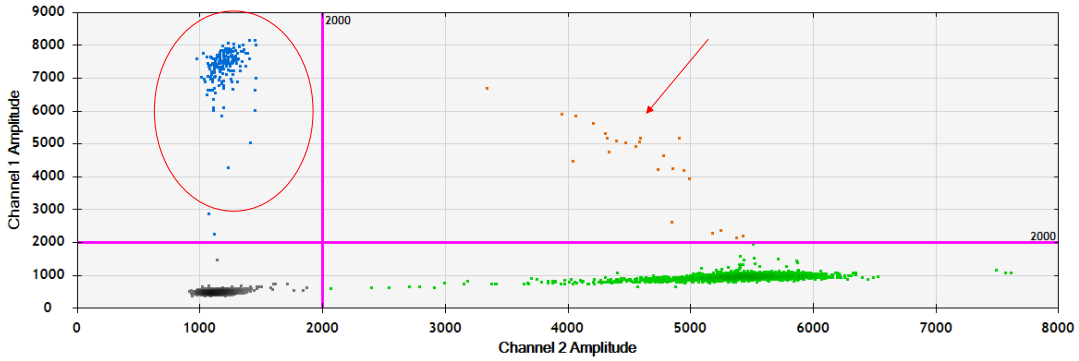

Figure 30 2D amplitude ddPCR plot for patient 3. Ch1+Ch2+: 24; Ch1+Ch2- : 177; Ch1-Ch2+: 4942; Ch1-Ch2-: 33640. A merge of 3 replicas of the patient 3 (6 µL each). A total of 18µL of the 50µL eluate was tested. Blue and orange dots show positive droplets for the mutation Mydd88 L265P. Green dots shows positive droplets for the WT molecule.

According with the clinical data of this patient diagnosed with Waldenstrom Macroglobulinemia, at the date of the sample, January 2018 the patient had an active disease showing IgM-levels of 6,8 G/L (figure 9S supplementary material).
Thus, the ddPCR results correlates well with the clinical data showing active disease.

Patient 4

In this patient, the ddPCR results showed 1 positive droplet for the mutation in the cluster Ch1+Ch2- (red circle in Figure 31) and positive droplets for the wild type probe. This corresponded to a concentration of 1,8 mutated and 2480 wild type copies in the PCR reaction (Table 4). The fractional abundance of this patient was 0,07% which is above the LoD, 0.05%.

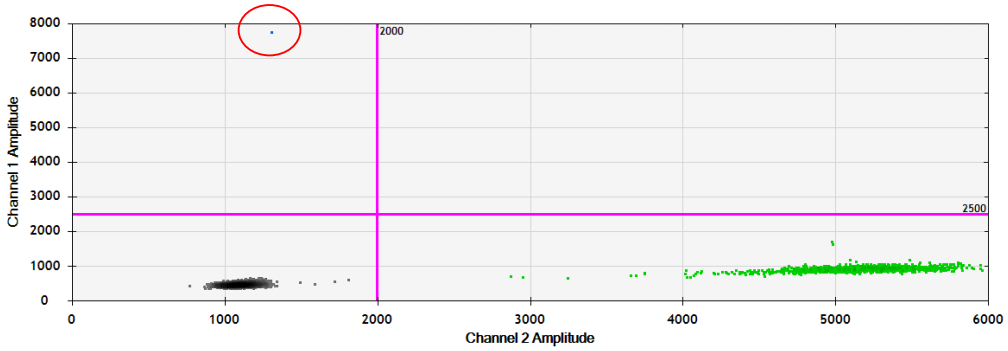

Figure 31. 2D amplitude ddPCR plot for patient 4. Ch1+Ch2+: 0; Ch1+Ch2- : 1; Ch1-Ch2+: 1353; Ch1-Ch2-: 37852. A merge of 3 replicas of the patient 3 (6 µL each). A total of 18µL of the 50µL eluate was tested. Blue dots shows positive droplets for the mutation Mydd88 L265P. Green dots shows positive droplets for the WT molecule.

According to these results, since the allele frequency was above the limit of detection, the droplet can be considered a true positive. However, the presence of only one positive droplet and the low fractional abundance, call into question the reliability of the positive FAM droplet. In order to be able to say with more certainty whether this patient is positive for the mutation, more patient sample would be recommended to analyze.

The clinical data for this patient diagnosed with Waldenstrom Macroglobulinemia, showed treatment stopped November 2017. At the time of the sample about a year later (October 2018) the patient was in for a control phase. At this moment the M-component curve was at its lowest although it still showed some abnormalities, IgM-lambda 7.5 G/L. (figure 9S Appendix).

The clinical data of this patient: a decreasing tendency of the M component curve and the IgM level at its lowest value, corelates with the uncertainty seen in the ddPCR results.

Patient 5

Digital droplet PCR results showed 2 positive droplets for the mutation in the Ch1+Ch2+ (red circle Figure 32) at a Ch1 amplitude of 3200, near to the threshold. Also, positive droplets for the wild type probe were detected. Following Poisson distribution, this corresponded to region a concentration of 5,8 mutated copies and 4340 WT copies in the PCR reaction, resulting in a fractional abundance of the mutated molecule of 0,13%, slightly above the LoD.

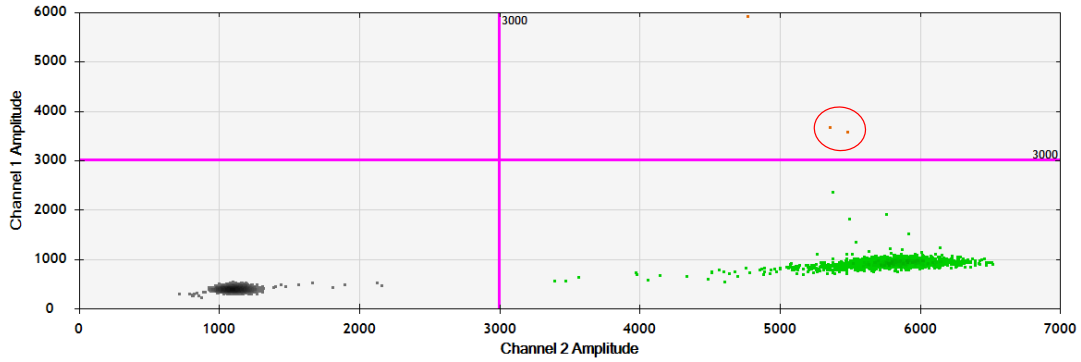

Figure 32 2D amplitude ddPCR plot for patient 5. Ch1+Ch2+: 3; Ch1+Ch2- : 0; Ch1-Ch2+: 2126; Ch1-Ch2-: 33605. A merge of 3 replicas of the patient 3 (6 µL each). A total of 18µL of the 50µL eluate was tested. Orange dots shows positive droplets for the mutation Mydd88 L265P and WT. Green dots shows positive droplets for the WT molecule.

According to these results, we can say that the 2 positive droplets are true positive since the fractional abundance is above the LoD of the assay, however, form this results it cannot be concluded with certainty if the patient had the mutation due to the low concentration abundance of the target molecule.

Looking at the clinical data, this patient, was diagnosed with IgM – MGUS. IgM levels at the date of sample were 2.5G/L (figure 9S supplementary material).

It is known that not all MGUS patient carry the mutation. Further screening of the patient sample could help to conclude the if the patient carries the mutation.

Patient 6

Digital droplet PCR results showed only 1 positive droplet for the mutation in the region Ch1+Ch2+ (red circle Figure 33) and several positive droplets for the wild type probe. This corresponded to a concentration of 2,2 mutated copies per and 4300 WT molecules in the PCR reaction. The mutant fractional abundance was 0,05% (Table 4).

The mutation rate of this patient is exactly the same as the Limit of detection, this together with the low Ch1 amplitude of the droplet, it cannot be concluded that this patient is either positive or negative for the mutation.

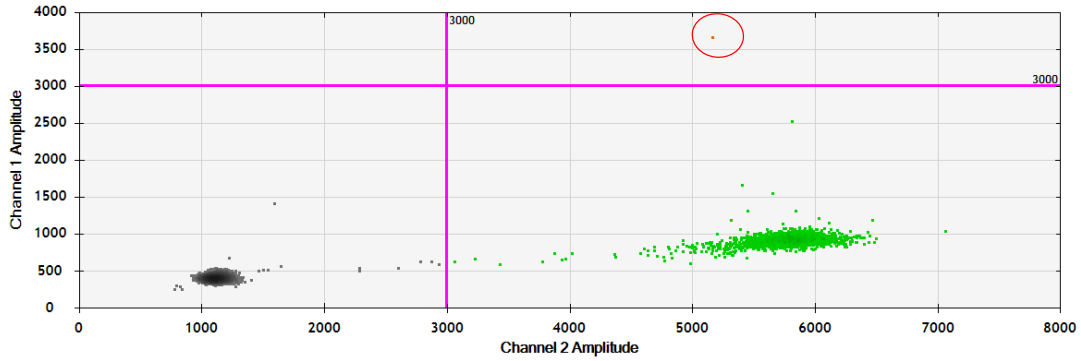

Figure 33 2D amplitude ddPCR plot for patient 6. Ch1+Ch2+: 1; Ch1+Ch2- : 0; Ch1-Ch2+: 1932; Ch1-Ch2-: 30803. A merge of 3 replicas of the patient 3 (6 µL each). A total of 18µL of the 50µL eluate was tested. Orange dots shows positive droplets for the mutation Mydd88 L265P and WT. Green dots shows positive droplets for the WT molecule.

The clinical data for this patient, diagnosed with Waldenstrom Macroglobulinemia, shows a IgM at the date of sample of 1 G/l and a decreasing tendency curve (figure 9S supplementary material.

Patient 7

The ddPCR results were negative for the mutation Myd88 L265P. No positive droplets for the mutated probe were found in the 18uL sample screened (Figure 34).

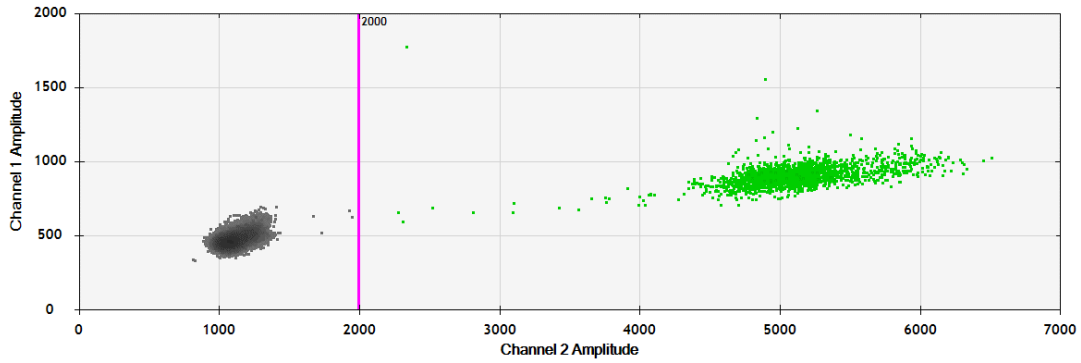

Figure 34 2D amplitude ddPCR plot for patient 7. Ch1+Ch2+: 0; Ch1+Ch2- : 0; Ch1-Ch2+: 1910; Ch1-Ch2-: 40858. No positive droplets for FAM detected.

Clinical data showed that this patient, diagnosed with Waldenstrom Macroglobulinemia, was currently receiving treatment with Imbruvica (ibrutinib) during the last 3 years, showing a good response to it. At the date of the extraction of the sample, the patient showed a normal M component curve, 0.1 G/L. (figure 9S supplementary material)

The results obtained from the ddPCR correlates with the clinical data, as this patient is a clear negative and the M component curve is normal.

Patient 8

The results of the ddPCR shows that the patient is negative for the mutation, not positive droplets for the mutation (FAM probe) found (Figure 35)

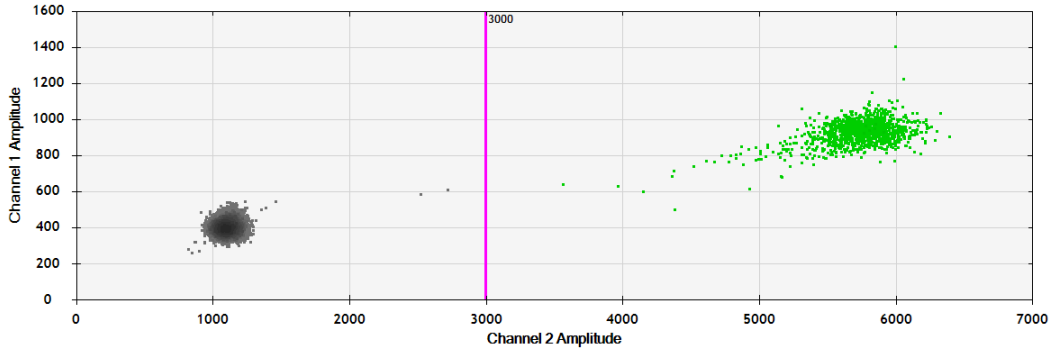

Figure 35 2D amplitude ddPCR plot for patient 8. Ch1+Ch2+: 0; Ch1+Ch2- : 0; Ch1-Ch2+: 1184; Ch1-Ch2-: 31774. No positive droplets for the mutation Mydd88 L265P.

Looking at the clinical data, this patient diagnosed with WM presented a decreasing M component curve with IgM value of 0,7 G/L (figure 9S supplementary material)
The clinical data of this patient corelates with the negative results of the digital droplet PCR for the mutation

M component and Myd88 L265P correlation

After the analysis of these 8 patients, the mutation was detected in cell free DNA of 6 patients. 2 patients had negative results for the mutation, clinical data suggested that these patients were in remission of the disease. When comparing the M component measurement (analyzed in the clinical lab) with the mutation detected by ddPCR a good correlation is found in most of the patients. In Figure 36 it is shown how some of the patients such as patient 2, 3, 5, 6, 7, and 8 showed a good correlation between both indictors, however, patient 1 and patient 4 presented very low levels of the mutation meanwhile they showed high IgM values.

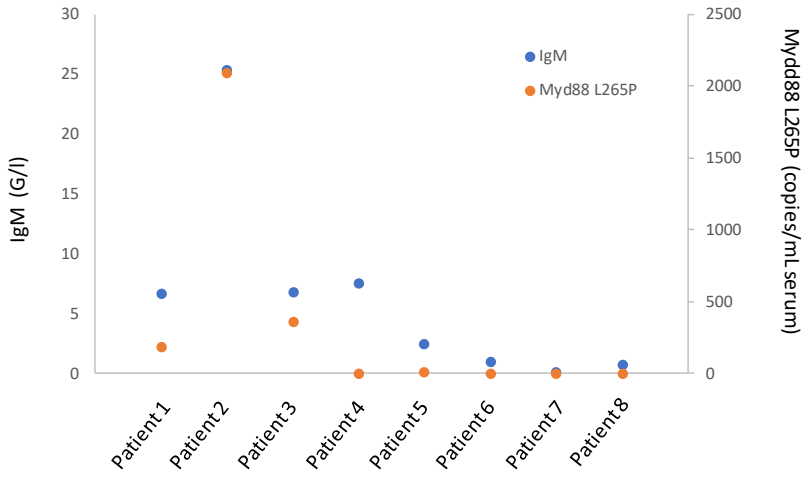

Figure 36. M component vs Myd88 L265P mutation. IgM levels of each patient plotted together with Myd88 L265P levels. The graph shows correlation between the 2 indicators in most of the patients. The negative patients showed also low levels of IgM.

Patient 9

19 samples from different timepoints, taken during a period of 9 years, were analyzed on the ddPCR, and compared to their corresponding M-component measurements (Table 5, Figure 37)

Timepoint	Fractional abundance (%)	Mut. copies / mL of serum	M component
9-1	1,3	116	68
9-2	1,3	103	63,59
9-3	6,4	214	53,5
9-4	2,1	156	55,6
9-5	0,6	130	51,9
9-6	3,0	131	50,8
9-7	1,8	62	51,6
9-8	0,2	106	57,3
9-9	1,3	104	59,3
9-10	1,1	97	64,7

Timepoint	Fractional abundance (%)	Mut. copies / mL of serum	M component
9-11	0,9	43	35,5
9-12	0,7	37	19,6
9-13	0	0	14,4
9-14	0	0	11,3
9-15	0	0	9,4
9-16	0	0	8,2
9-17	0	0	7,3
9-18	0,5	16	17,5
9-19	1,0	44	22,8

Table 5 Digital droplet PCR results and M component value for 19 time points from samples taken from 2009 to 2019. Mutated copies refer to the mutation (Myd88 L265P).

There is an overall good correlation between the M components levels and the mutation detected, however, some samples deviates from the curve. The decrease of IgM in March 2011 is followed also by the decrease of the mutation levels. However, it can be noticed that in 5 samples no mutation is found meanwhile IgM levels are not down to 0 G/L. This reflects that the M component could be a bit more sensitive for disease monitoring than Myd88 mutation detection by ddPCR mutation detection or that posible errors during serum sampling could lower the sensitivity of the droplet assay.

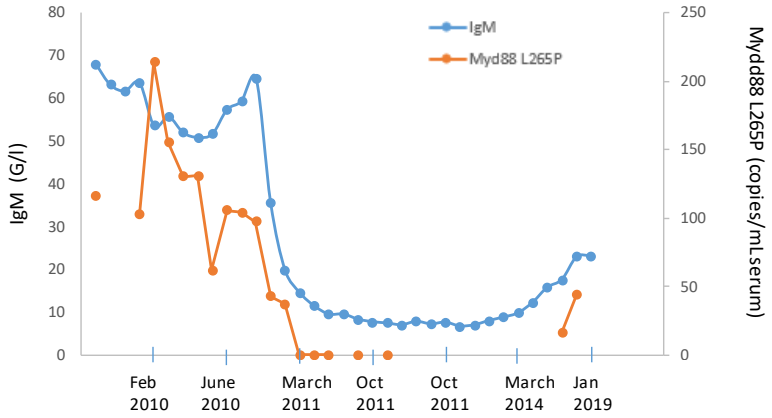

Figure 37 ddPCR results vs IgM (M component). Both curves follow a similar pattern, although IgM seems to be more sensitive than Myd88 mutation

The clinical data for this Waldenstrom patient, diagnosed in December 2009 (when the first sample was taken), shows IgM values of 68 G/L at diagnosis. The patient was treated and it stopped in march 2010. Second line treatment was given due to increased M component in 2011 and following that the M component decreased to its lowest values.

The patient remains untreated until the last control at 17 January 2019. Looking at the ddPCR results and M component levels we could say that the patient is in a progression stage, according to the last positive samples and increasing serum IgM.

4.2. Hairy Cell Leukemia

Limit of Detection and False positive rate

For the analysis of HCL, the mutation BRAF V600E was targeted. The LoD test was performed using serial dilutions 1:4 of the mutant target (HT29). Table 6 lists the theoretical and acquired number of copies in the LoD experiment (per PCR reaction).

		Expected results		Experimental results		
Dilutions and controls	**HT29 copies***	25% BRAF V600E	75% WT + gDNA copies	**Mutated copies**	**WT copies***	**Fractional abundance (%)**
1:1	3636	909,0	6363	966,0	5520	14,90
1:4	909	227,3	4318	244,0	3980	5,80
1:16	227	56,8	3806	66,0	3340	1,92
1:64	57	14,2	3679	13,4	2900	0,46
1:256	14	3,6	3647	5,0	3400	0,15
1:1024	4	0,9	3639	0	3180	0
NC (wt)	0	0	3636	0	2904	0
PC	3636	909	2727	1086	3140	-
NTC	0	0	0	0	0	-

Table 6 BRAF V600E LoD results. Theoretical and acquired number of copies across the different dilutions. Copies are given in the 20µL PCR reaction. The HT29 cell line, used as positive control and mutated target for the dilutions is heterozygous for the mutation. 25% of the alleles carry the mutation and 75% are WT according with the results obtained. NC: negative control; PC: positive control; NTC: non template control.

As we previously described in chapter 3.4.2. The cell line HT29 used as positive control and as mutant target, is heterozygous for the mutation BRAF V600E. Thus, in this case, ddPCR results of the LoD does not shown a constant Wild Type background because HT29 also has WT molecules (Figure 38). The mutated copies decrease according to the theoretical dilution curve as confirmed by a R-squared value of 0,99 (Figure 39).

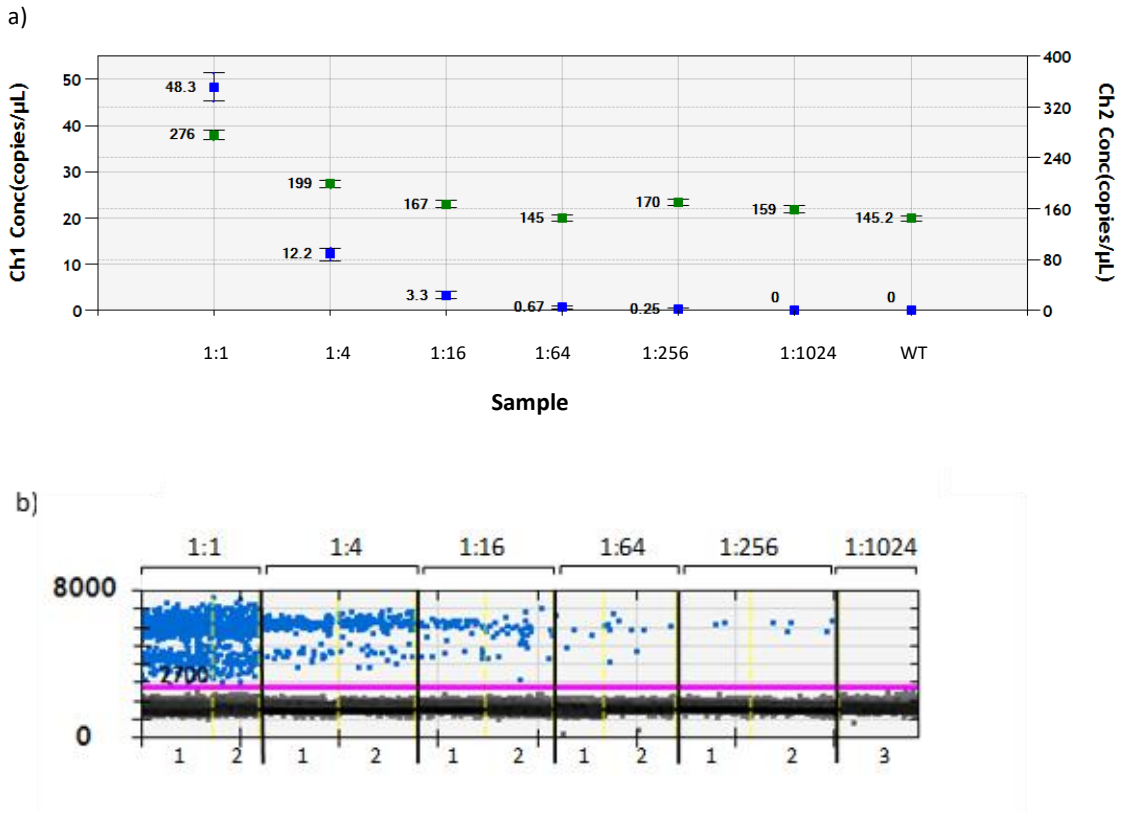

Figure 38 BRAF Dilution test for the determination of the LoD. **a)** Green square - Wild Type concentration (HEX), The WT background doesn't remain constant because the mutant, HT29 cell line carry also wild type molecules. Blue square - mutant concentration, it decreases according to the serial dilutions. Negative controls (WT) and none template controls (NTC) shows no false positive droplets. **b)** 1D amplitude ddPCR plot of the different replicates per dilution. Blue dots are positive droplets for the mutation (FAM).

The FPR was acquired according to the three negative controls (WT) of the experiment. It was found to be 0% but the upper 95% CI was 1,6 copies per PCR reaction. Thus, combining the dilution curve, the false positive rate and its 95% CI the limit of detection for this assay is set at an allele frequency of 0.15% meaning that 7 copies can be reliable called true positive in a background of 5.000 WT molecules. When applied to patient samples, those with a mutation rate above the LoD 0.15% were considered true positive.

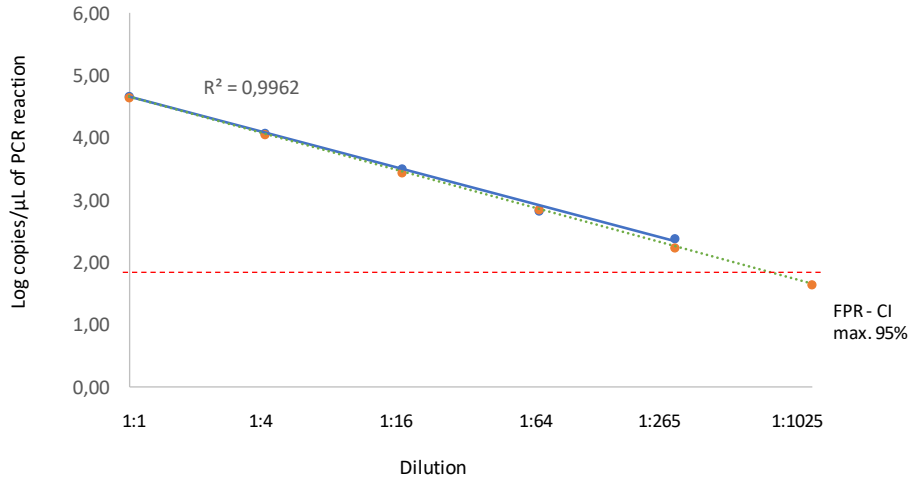

Figure 39. Limit of Detection BRAF V600E assay. The graphic shows $\log_{10}$ of the mutated concentration (copy number per µL of ddPCR reaction) plotted against the corresponding dilutions. Blue line – experimental results. Green dotted line – expected results. The curve is transformed into a linear regression, being R^2= 0,99. The red line shows the false positive rate based 3 wild type controls. The dotted red line shows the Poisson 95% CI of the FPR. The LoD, was determined based on the upper value of the 95% confidence interval of the false positive rate

Patients samples

Two patients diagnosed with Hairy Cell Leukemia were tested for the BRAF V600E mutation. One of the patients had only one sample, while and the other patient had 3 samples taken at different timepoints during a 2-year period (Table 1). In all of the patients 3 replicas of 6µL of sample were performed and showed as a merge, thus, a total of 18µL of eluate per patient was analyzed.

First, a mix of cfDNA from 9 healthy donors (HD) in 8 replicates was analyzed in order to test if the mutation BRAF V600P could be found in healthy donors or it was specific for patients Figure 40. No positive droplets positive for the mutation were found according to the threshold previously established at 3000/2500 amplitude (Ch1/Ch2) (as explained in section 3.3.5).

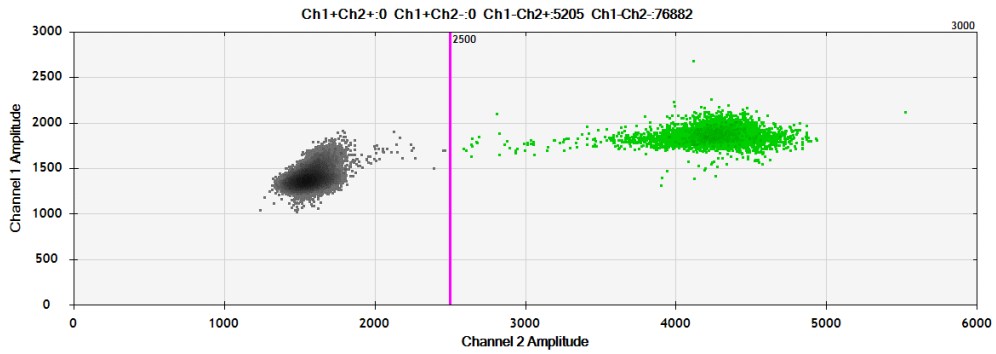

Figure 40 2D amplitude ddPCR plot for healthy donor merge. Ch1+Ch2+: 0; Ch1+Ch2- : 0; Ch1-Ch2+: 5357; Ch1-Ch2-: 85101. No positive droplets for the mutation are found.

Patient 10

The ddPCR results shows that this patient is negative for the mutation BRAF V6000E. No positive droplets for FAM probe were found in the 18uL sample screened (Figure 41).

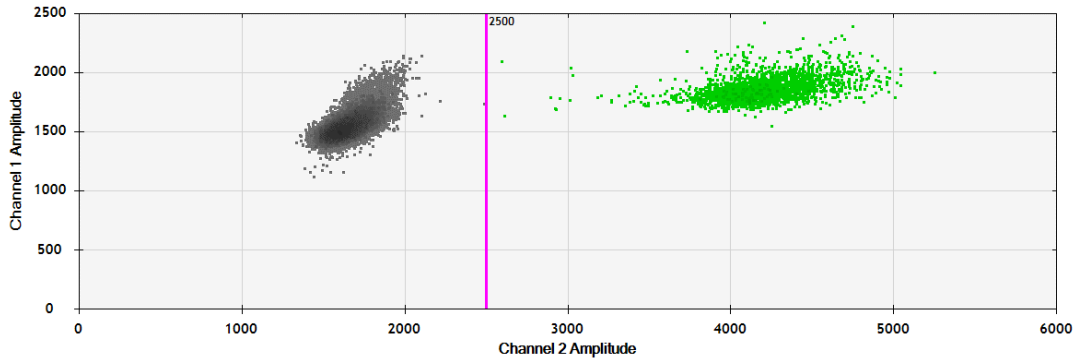

Figure 41 2D amplitude ddPCR plot for patient 10. Ch1+Ch2+: 0; Ch1+Ch2- : 0; Ch1-Ch2+: 2672; Ch1-Ch2-: 28589. No positive droplets for the mutation are detected.

Looking at the clinical data, this patient was diagnosed with Hairy Cell Leukemia in 2013 and bone marrow biopsy at diagnosis showed BRAF V600E mutation. At the time of sample extraction 5 years later (Oct 2018), the patient had responded well to treatment and had not received treatment since March.

Thus, ddPCR results and clinical data could correlate since this patient could have been cured.

Patient 11

3 samples from different timepoints were tested. The ddPCR results after screening 18 µL of each eluate showed 1 positive droplet for the mutation in Ch1+Ch2- cluster in the

first two samples, (Figure 42 a) and b)). The third sample, showed one positive droplet for both, the mutation and wild type, Ch1+Ch2+ cluster (Figure 42 c)).

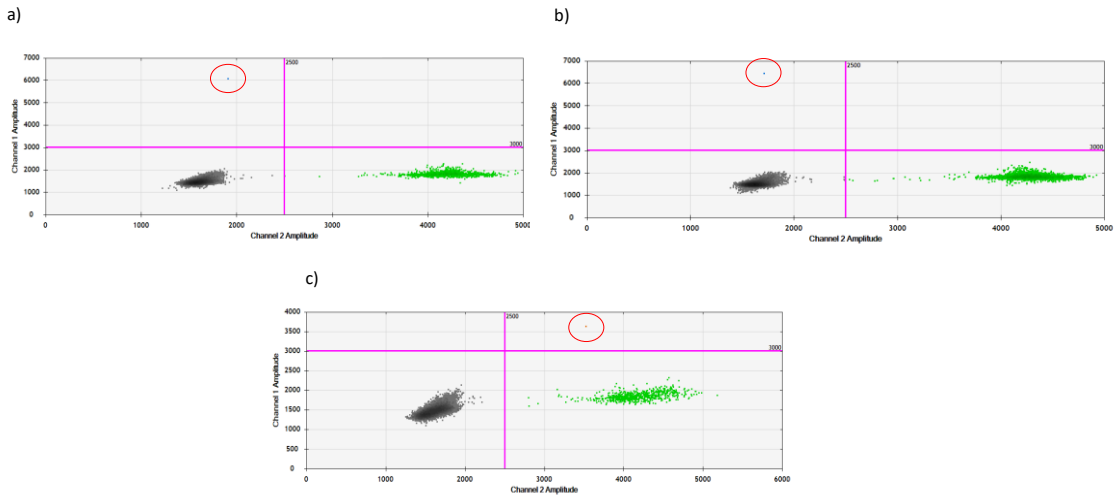

Figure 42 2D amplitude ddPCR plot for patient 11. a) Date of sample April 2017. Ch1+Ch2+: 0; Ch1+Ch2- : 1; Ch1-Ch2+: 1428; Ch1-Ch2-: 27009. One positive droplet for the mutation is detected (red circle). b) Date of sample April 2018. Ch1+Ch2+: 0; Ch1+Ch2-: 1; Ch1-Ch2+: 5828; Ch1-Ch2-: 32061 One positive droplet for the mutation is detected (red circle). c) Date of sample October 2018, Ch1+Ch2+: 1; Ch1+Ch2- : 0; Ch1-Ch2+: 711; Ch1-Ch2-: 28887. One positive droplet for both, FAM and HEX probe is found.

Table 7 shows the concentration of mutated molecules (according with Poisson distribution) in each sample and its fractional abundance. Since the concentration is very low and just one positive droplet for the mutation was found to be positive in each sample, it cannot be said with certainty that the samples are positive for the mutation. Besides, the LoD of the assay was stablished at 0,15%, and as we can see in Table 7, the three samples have a fractional abundance below the LoD. Thus, we could conclude that the positive droplets for the mutation could be false positive since they are under the LoD of the assay and that all samples are negative for the mutation.

	In 18µL of eluate tested			
Patient (sample)	**Mutated copies/PCR reaction**	**WT copies/PCR reaction**	**Fractional abundance (%)**	**Mutated copies/mL serum**
11-1	0,8	572	0,14	4
11-2	0,8	1212	0,07	5
11-3	0,6	3920	0,015	4

Table 7 Overview of the mutated copies and fractional abundance. All of the samples have a fractional abundance below the Limit of Detection of the assay, 0,15%

Looking at the clinical data, this patient was diagnosed with Hairy Cell Leukemia in 2004 and since then the patient had 4 relapses. The last treatment to which the patient had a good response ended in august 2015. At the point of the samples tested that patient showed a good response to treatment with normal blood test values.
Thus, it is not known whether the patient is cured, and no longer have cancer cells present, or if there still are cancer cells present that will lead to a later relapse.

4.3. Acute Promyelocytic Leukemia

Limit of Detection and False positive rate

For the study of the translocation PML-RARA, two transcripts of the translocation were considered, Bcr1_2 and Bcr3, thus two different Limit of Detections were done.
The Limit of Detection test was performed in a similar way as for the other two malignances, doing 1:4 serial dilutions. The positive copies used for the dilutions was the gene Block showed in Figure 6S in Appendix (see section 3.4.20 Controls). Table 8 lists the theoretical and acquired number of copies in the LoD experiment (per PCR reaction).

a) **Transcript Bcr1_2**

	Expected results		Experimental results		
Dilutions and controls	**Mutated copies***	**WT copies***	**Mutated copies***	**WT copies***	**Fractional abundance (%)**
1:1	3000	3636	3220,0	3480	48,00
1:4	750	3636	678,0	3460	16,40
1:16	189	3636	188,0	3462	5,10
1:64	48	3636	40,8	3680	1,10
1:256	12	3636	5,0	3208	0,16
1:1024	3	3636	1,8	3274	0,06
NC (wt)	0	3636	0	3140	-
PC	3000	0	2952	0	-
NTC	0	0	0	0	-

b) **Transcript Bcr3**

	Expected results		Experimental results		
Dilutions and controls	**Mutated copies***	**WT copies***	**Mutated copies***	**WT copies***	**Fractional abundance (%)**
1:1	3000	3636	4400	3064	59,40
1:4	750	3636	964	3576	21,80
1:16	189	3636	250	3282	7,10
1:64	48	3636	64	3000	2,11
1:256	12	3636	17,6	3400	0,53
1:1024	3	3636	6,8	3526	0,19
NC (wt)	0	3636	0	3430	-
PC	3000	0		0	-
NTC	0	0	0	0	-

Table 8. PML-RARA LoD results. Theoretical and acquired number of copies across the different dilutions. *Copies in the 20µL PCR reaction. NC: negative control; PC: positive control. **a)** Transcript Bcr1_2 results. Expected results corelates with the obtained ones. **b)** Transcript Bcr3 results. The primer Bcr3 was added to the assay. The mutated copy number obtained was slightly above the expected ones

The wild type background remains stable, and the mutated copies decrease according to the theoretical dilution curve (Figure 43), as confirmed by a R-squared value of 0,99 in both transcripts (Figure 44***Figure 26***).

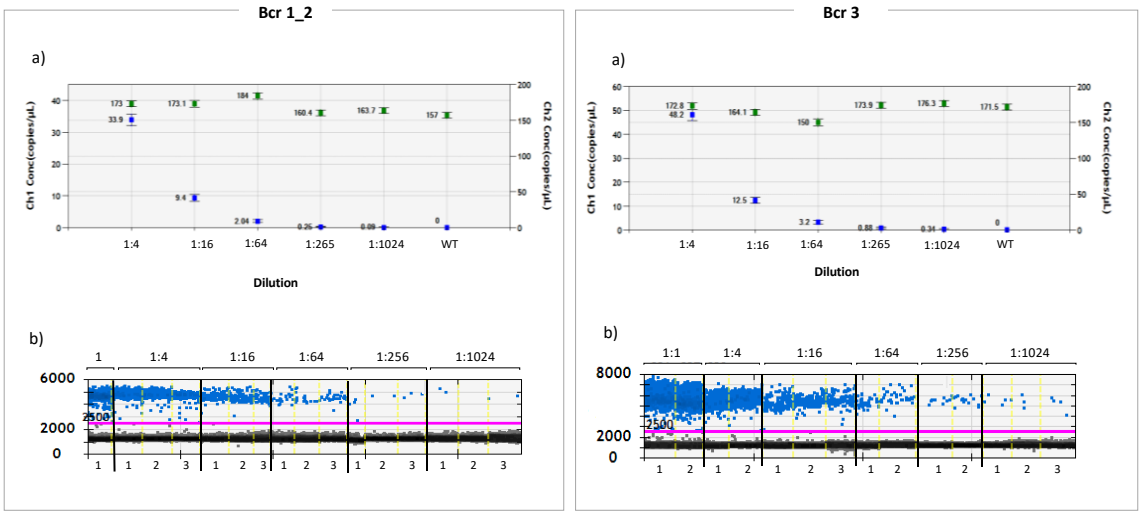

Figure 43 Dilution tests for the determination of the LoD. Bcr 1_2 and Bcr 3. a) Green square - Wild Type concentration (HEX) remains constant in both LoD. Blue square - mutant concentration, decrease according to the serial dilutions (mutant + genomic DNA). Negative controls (WT) and NTC shows no false positive droplets. The first dilution is skip in both graphic in order to show better the lower dilutions. **b)** 1D amplitude ddPCR plot of the different replicates per dilution. Blue dots are positive droplets for the mutation (FAM).

Bcr 1_2: The false positive rate was found to be 0 cp/reaction, and the upper 95% CI of the WT control was found to be 0,075 cp/µL of PCR reaction, thus, to determine the LoD, the first dilution that is above the upper 95% CI was 1:1024. In this dilution we were able to detect mutated copies in a WT background at a fractional abundance of 0,06% (LoD), in other words we can detect with reliability 6 mutated copies in a background of 10.000 WT molecules. Results below this LoD cannot be consider true positive.

Bcr 3: In this case the FPR was 0cp/reaction and the upper 95% CI of the WT control was established at 0,077 cp/µL of PCR reaction. The first dilution above the FPR was also the 1:1024, in which we were able to detect mutated copies at a fractional abundance of 0,19%. Thus, the LoD of this assay was 10 mutated copies in a background of 5.000 WT molecules. Everything below this LoD cannot be consider a true positive with certainty.

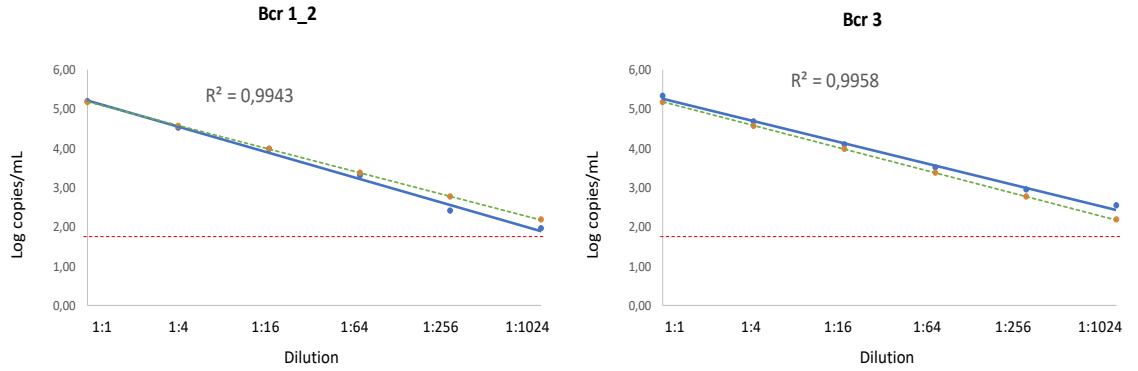

Figure 44 Limit of Detection PML-RARA Bcr 1_2 and Bcr 3 assay. The graphic shows $\log_{10}$ of the mutated concentration (copy number per µL of ddPCR reaction) plotted against the corresponding dilutions. Blue line – experimental results. Green dotted line – expected results. The curve is transformed into a linear regression, being in both Bcr1_2 and Bcr 3, R^2= 0,99. The dotted red line shows the Poisson 95% CI of the FPR.

Patient samples

Since the breaking point in gene RARA occurs within an intron (see Figure 9 in section 1.3.3. Acute promyelocytic leukemia), in order to obtain product after PCR amplification, ctRNA (where splicing and removal of introns have taken place) is chosen for the analysis instead of cfDNA. Prior to test patient samples, we tested whether we were able to isolate cfRNA using the same kit as for cfDNA and without following any extra step to avoid RNA degradation. To test this, 2 experiments were performed with different primers in cfRNA from 2 healthy donors in each of the experiment.

Bcr1_2 assay: Assay used for the LoD. As explained in section 3.4.1. Assays – primer / probes, the WT assay (HEX probe) amplifies the exon 2 in PML gene. This fragment will be amplified in all wild type molecules. The mutated assay (FAM probe) will amplify the translocation. Healthy donors are expected to be negative for the mutated assay. The results are shown in Figure 45.

Bcr1_2 assay + primer RARA exon 2: To the primers in the Bcr1_2 assay another primer in the exon 2 in RARA gen was added (see section 3.4.1. Assays – primer / probes,

61 ttctcctggg aaccccatcg gccccctgcc agcacacacc tgagcagcat cacaggacat

```
121 ggccccctca gccacctagc tggggcccat ctaggagtgg catcttttt ggtgccctga
181 aggccagctc tggaccttcc caggaaaagt gccagctcac agaactgctt gaccaaagga
241 ccggctcttg agacatcccc caacccacct ggcccccagc tagggtgggg gctccaggag
301 actgagatta gcctgccctc tttggacagc agctccagga cagggcgggt gggctgacca
361 cccaaacccc atctgggccc aggccccatg ccccgaggag gggtggtctg aagcccacca
421 gagccccctg ccagactgtc tgcctccctt ctgactgtgg ccgcttggca tggccagcaa
481 cagcagctcc tgcccgacac ctgggggcgg gcacctcaat gggtacccgg tgcctcccta
```

```
541 cgccttcttc ttccccccta tgctgggtgg actctccccg ccaggcgctc tgaccactct
601 ccagcaccag cttccagtta gtggatatag cacaccatcc ccagccacca ttgagaccca
```

Figure 20). The same WT (HEX) region will be amplified but, in this case, the new primer together with the other reverse primer in the mutated assay (FAM) located in exon 3 of RARA gene will give product in the case of having cfRNA. Since there is a big intron sequence between both primers, just mature RNA free of introns will give product. Results are shown in Figure 45.

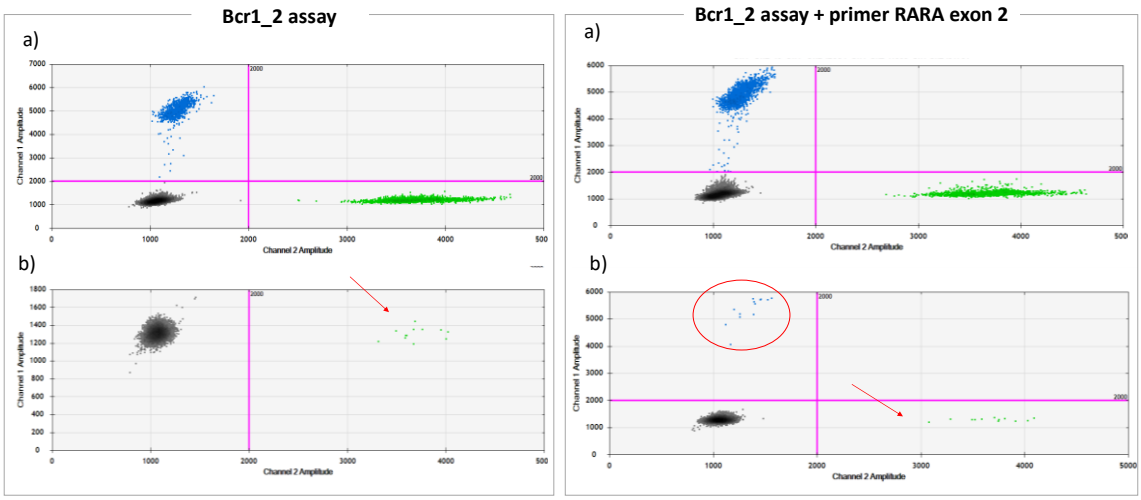

Figure 45 2D ddPCR plot. cfRNA form healthy donors tested with 2 different primers. a) Shows the controls and threshold. b) shows the mutated and WT copies detected in the cfRNA from the 2 healthy donors. **Bcr1_2:** there is HEX amplification (arrow) corresponding to the exon 2 of PML, but no FAM signal as expected, since the primers are amplifying the translocation and just healthy donors are being tested. **Bcr1_2 assay + primer RARA exon 2:** there is HEX amplification (arrow) corresponding to the exon 2 of PML and there is also FAM amplification (red circle). The new primer in exon 2 of RARA give product together with the primer in exon 3 of RARA.

The positive results for FAM in the Bcr1_2 assay + primer RARA exon 2 experiment suggested that cfRNA was being analysed since the only way to obtain product was if the introns were not present. However, the amount of copies obtained was too low; 6,4 and 9,4 copies in the reaction for FAM probe and 6,4 and 8,2 for HEX probe (for each of the healthy donors). Both HD have almost the same amount of FAM/HEX copies since both probes targeted wild type copies. Thus, it can be concluded that it is possible to isolate cfRNA with QIAamp Circulating Nucleic Acid Kit but the concentration obtained is very low (it may be degraded before the ddPCR experiments).

Patients samples

Two patients with APL were provided for its analysis, see Table 1. However, due to low cfRNA yields obtained in the control experiments, the analysis of these samples was postponed until a better protocol for cfRNA preservation and isolation is found.

5. Discussion

The discovery of cell free nucleic acids (cfDNA/cfRNA) and more specific circulating tumor DNA (ctDNA) in blood has led to the concept of "liquid biopsy". As ctDNA molecules carry the mutations present in the cancer cells, its detection and analysis can be used as a non-invasive, rapid and painless method for cancer biopsy. However, the detection of ctDNA can be challenging due to its low concentration in blood. Thus, platforms such as digital droplet PCR have allowed its detection with high sensitivity and specificity.

This master thesis describes the validation of three ddPCR assays for three different mutations and their detection using ddPCR in patients carrying the genetic alteration.

When working with cfDNA, as we have previously described, it's usually recommended to isolate it from plasma rather than serum (54). One of the reasons is that when processing a serum sample for its use in cfDNA analysis, cfDNA can be contaminated with genomic DNA released by the accidentally breakage of leucocytes during the clotting formation. Thus, the cfDNA would be diluted by high amounts of genomic DNA making more difficult the detection of the target molecule. Some of the cfDNA samples included in the study had high concentration of DNA. These patient samples (9-5, 9-6, 9-8 and 11) were analyzed in an Agilent chip. The three samples of patient 9 showed genomic DNA contamination. However, the ddPCR results of these patient seemed normal (Table 5).

Several biobanks (such as the Janus bank) have stored serum samples, thus trying to find ctDNA in serum samples of patients is of great interest. In this project serum samples were used, in order to check if serum is optimal sample for ctDNA isolation. According to the results obtained, it can be concluded that cfDNA can be isolated from serum, however, further research should be done to test whether plasma samples can provide better cfDNA yields than serum and also considering different volume samples.

In this study it has been shown that the mutation Myd88 L265P can be detected in ctDNA. This has been also demonstrated in other publications (24). In this project, it has been also shown the correlation between the mutation Myd88 L265P and the M component in patients with Waldenstrom Macroglobulinemia. This can be seen in patients 1 to 8 and in patient 9 across the different 19 timepoints. It is seen that when ddPCR results are negative for the mutation, the M component is slightly above 0, suggesting that the

detection of the last indicator (M component) can me a bit more accurate in patients/timepoints with low disease burden. The correlation between a specific mutation and the M component has been described in other publications and in other diseases such as Multiple Myeloma (65), however, this has still not been described for WM. From the results in this thesis it could be conclude that the detection of the monoclonal IgM could be slightly more sensitive method in patients with low tumor burden, although more samples are needed to verify this. As it can be seen in Figure 40, the M component levels start to increase (March 2014) before we see positive results for the mutation. In those patients were it seems that the correlation is lower, as is the case of patient 1 in Figure 40 it can be due to fact that the M component is not always produced to the same extend in all tumors and that's why the use of a comparable method can be useful to complete the analysis.

The early detection of the mutation will not make the treatment to start earlier, according to the current management of the disease, treatment will not start until the patient have symptoms (22). However, some mutations also found in WM patients such as those in the gen CXCR4 are resistant to some treatments (21). Thus, knowing the molecular profile of the patient can help to give the adequate treatment to each patient. Novel approaches in the treatment of WM suggest the use of BTK inhibitors (Bruton Tyrosine Kinase), such as ibrutinib. BTK is a kinase in the toll like receptor cascade involved in the phosphorylation of IRAK4 after Myd88 activation and dimerization (see Figure 4). Thus, the detection of the mutation Myd88 could influence the choice of treatment since patients Myd88 (WT) are not responsive to this drug (70). Besides the detection of the Myd88 mutation could help with the differential diagnosis of other malignancies such as IgM – Multiple Myeloma (21) .

Clear conclusions from HCL patients cannot be made since only samples from two patients with HCL were received. All the samples were concluded to be negative for the mutation since the number of mutated copies detected was below the limit of detection of the assay. The clinical data of these two patients showed they were on remission of the disease, thus, data obtained could be trustfully considering clinical data. Other publications describe the detection of the mutation using ddPCR in cells from HCL patients (37) and the detection of BRAF V600E in ctDNA from melanoma patients (71). Due to the low number of patients/samples tested, it cannot be conclude whether the mutation can be detected in HCL patients or not using ddPCR. Thus, for further research,

HCL patient with an active disease should be tested. Besides, in the case of HCL, the presence of the mutation in BRAF gene implies therapeutic advantages, since the mutation can be target for BRAF (kinase) inhibitors drugs, suggesting that the early detection of the mutation could make treatment start earlier un thus, obtain better results for the patient.

One of the limitations of the project was the lack of a standardized protocol for the isolation of cfRNA with high efficacy. When the assay for PML-RARA was planned (primer/probes sequences from a previous published paper), it was thought to be used in cfDNA. However, as it is represented in Figure 9 and in section 3.4.1. Assays – primer/probe design, the primers were spanning large introns. When considering translocations, the detection of the mutation in genomic DNA by PCR is sometimes impeded by extremely large intron sequences flanking the breaking point regions. Thus, a better target could be the transcript (mRNA), once the maturation process of the DNA takes place, as we get rid of large intronic regions (72). There are several studies where the transcript PML-RARA was analyzed using ddPCR in RNA isolated from cells (42, 73, 74). This implies that for the detection of the transcript, ctRNA should to be isolated instead of ctDNA. We were able to detect cfRNA in this project, however, the sensitivity was pretty low, making it difficult to be able to detect circulating tumor RNA. Although the QIAamp Circulating Nucleic Acid Kit used for ctDNA isolation can be used also for the isolation of ctRNA, as tested in this project, the lack of a well standardized protocol for handling RNA and the lack of any method used to conserve the RNA from blood extraction to ctRNA isolation might have contributed to the limitations.

In the literature, it is described that one of the methods to keep cfRNA stable is adding Trizol after the plasma or serum sample is processed and before it is frozen at -80 (75, 76). Besides, it has been reported that circulating microvesicles, exosomes, and apoptotic bodies can be a more stable source of RNA molecules, since it is protected from RNAses and degradation (57).

Thus, for further research in cfRNA, first a good protocol for its conservation should be followed. Besides it could be test whether the ctRNA is degraded in the isolation step by adding a known amount of an RNA standard into a serum sample, and measure it after the ctRNA isolation of the serum sample.

In the case of APL patients, the treatment with ATRA has been very successful and since the main treatment of the disease is directly targeted towards the translocation, its early detection is important for the success of the treatment and prognosis of the disease (48).

Digital droplet PCR can give more sensitive results that other techniques, thanks to its principle of sample partitioning. The results in this project showed that ddPCR had a good sensitivity around 0,05% and 0,15% depending on the assay, superior to other techniques such as allele-specific polymerase chain reaction (24). According to the results in this project, only clear results (either positive or negative) we made for 5 out of the 9 Waldenstrom patients and 1 out of 2 HCL patient (Table 4). The rest of the patients had ambiguous results. With this results, it could be said that the use of ddPCR in the clinical routine for diagnosis can be questionable, however it could be used for monitoring of the patients since some of this disease (WM and HCL) a not curable but the good response to some treatments such as in HCL can make the patient be in complete remission for years until relapse. Moreover, in this diseases the same mutation is present in all the course of the disease (form diagnosis until relapse), so the mutation could be easily monitored. Besides as we have previously discussed, the early detection of these mutations could have therapeutically advantages (allowing treatment start earlier such as in HCL and APL) or it can have a therapeutic benefit for future therapies in WM patients.

When comparing ddPCR with other sensitive techniques such as NGS for the analysis cfDNA, one of the main drawbacks of digital PCR is the low target abundance in the sample that can limit the detection and that ddPCR can only work with known mutations (it needs known primer and probes) (77). However, ddPCR is quicker, easy to use, cheaper and needs less bioinformatic, what makes this method a good tool to include it in the future clinical practice.

As previously discussed, there is an interest of knowing how early a mutation can be detected in an individual before symptoms and diagnosis appear (either for diagnosis, treatment improvement, or just biological interest). However, the data obtained suggested that the detection of ctDNA using ddPCR is not sensitive enough to detect mutations in non-active diseases. All of the patient samples tested that were in remission or with no-active disease have been negative even at volumes higher than 1mL meaning that in lower volumes such those form Janus bank (0.5mL) and in samples that are not reported to have an active disease at the time of the sample would be unlikely to detect the mutation.

Besides it is known, and as the data in this project shows (Table 4), that cfDNA concentration has a high variability from individual to individual and from patients with different stage of the disease, so it may be that the condition of the patient (for instance if it has an active disease or not) is more relevant for ctDNA yields rather than the volume of the sample itself.

Regarding the methodological part of the project, the LoD and FPR could have been improved. Tthe false positive rate (FPR) for each Limit of Detection was based in 3 wild type (negative controls) and no false positive droplets were found in any of the assays. However, the more WT samples are tested the higher chances to find a false positive, thus, increasing the number of WT sample tested we could have come up with a more specific LoD.

Another point to comment regarding the validation of the assays is that the ddPCR protocol suggest an annealing temperature of 55ºC, however, each assay is supposed to have an optimate annealing temperature. For the validation of the assays in this project the annealing temperature was not optimized for each assay. Doing that optimization, a better performance of the assay could have been obtained.

6. Conclusion and further perspective

The goal of the thesis was to get through aim 1-4, however, the need for testing cfRNA isolation was an unexpected event, leading to lack of time for aim 4

1. Three assays for digital droplet PCR platform were successfully validated. The Limit of Detection, as well as the false positive rate was found to be good enough for each assay. The LoD results had a good linearity and experimental results were quite similar to the expected ones.
2. Myd88 L265P and BRAF V600E mutations were tested with ddPCR in Waldenstrom Macroglobulinemia and Hairy Cell Leukemia patients obtaining results that were concordant with their clinical data. The translocation PML-RARA could not be tested in patients due to the lack of a standardized protocol to conserve and isolate cfRNA in an effective way. For the test of the translocation in cfRNA a better protocol should be followed.
3. A good correlation was obtained between Myd88 L265P and monoclonal IgM serum levels.

It can be concluded that ctDNA (liquid biopsy) could be a good biomarker for some diseases for instance Waldenstrom Macroglobulinemia and that ddPCR is a sensitive technique for its detection, it was able to detect Myd88 L265P mutations with high accuracy compare to other methods such as M component measurement. However, the results cannot be extrapolated to other hematological malignancies since the validation of a specific assay is needed.

For further study of APL samples, a functioning protocol to detect the PML-RARA translocation in circulating tumor nucleic acids should be found.
Moreover, HCL patients with an active disease should be tested in order to conclude if the ddPCR and the assay worked successfully in these patients.

In general, more patients with both, an active and non-active disease should be tested in order to elucidate if it is possible to find any of the mutations in patients with a non-active disease.

Bibliography

1. (WHO) Iafroc. 12 September 2018 [Available from: https://www.who.int/cancer/PRGlobocanFinal.pdf.
2. (WHO) WHO. Cancer 2019 [07/05/2019]. Available from: https://www.who.int/cancer/en/.
3. Dagogo-Jack I, Shaw AT. Tumour heterogeneity and resistance to cancer therapies. Nat Rev Clin Oncol. 2018;15(2):81-94.
4. Knudson AG. Hereditary cancer: Two hits revisited. Journal of Cancer Research and Clinical Oncology. March 1996;122(3):135–40.
5. Berk HLA, Zipursky SL, Matsudaira P, Baltimore D, Darnell. J. Molecular Cell Biology. 4th edition. In: Freeman; WH, editor. New York.
6. McGranahan N, Swanton C. Clonal Heterogeneity and Tumor Evolution: Past, Present, and the Future. Cell. 2017;168(4):613-28.
7. (NHI) NCI. NCI Dictionary of Cancer Terms. US Department of Health and Human Services. 2019.
8. Krok-Schoen JL, Fisher JL, Stephens JA, Mims A, Ayyappan S, Woyach JA, et al. Incidence and survival of hematological cancers among adults ages >/=75 years. Cancer Med. 2018.
9. Norway Cri. Cancer incidence, mortality, survival, and prevalence in Norway. 2017.
10. Ackermann M, Liebhaber S, Klusmann JH, Lachmann N. Lost in translation: pluripotent stem cell-derived hematopoiesis. EMBO Mol Med. 2015;7(11):1388-402.
11. Kondo M. Lymphoid and myeloid lineage commitment in multipotent hematopoietic progenitors. Immunol Rev. 2010;238(1):37-46.
12. Wang H, Leng Y, Gong Y. Bone Marrow Fat and Hematopoiesis. Front Endocrinol (Lausanne). 2018;9:694.
13. Abel AM, Yang C, Thakar MS, Malarkannan S. Natural Killer Cells: Development, Maturation, and Clinical Utilization. Front Immunol. 2018;9:1869.
14. LeBien TW, Tedder TF. B lymphocytes: how they develop and function. Blood. 2008;112(5):1570-80.
15. Kumar BV, Connors TJ, Farber DL. Human T Cell Development, Localization, and Function throughout Life. Immunity. 2018;48(2):202-13.
16. Klausner R. Leukemia, Lymphoma, and Multiple Myeloma: Toward a New Understanding. National Cancer Institute, Washington. 2001.
17. Palumbo A, Kenneth Anderson MD. Multiple Myeloma. The new england journal of medicine. 2011;364:1046-60.
18. Janz S. Waldenstrom macroglobulinemia: clinical and immunological aspects, natural history, cell of origin, and emerging mouse models. ISRN Hematol. 2013;2013:815325.
19. Olsen M. Overview of Hematologic Malignancies. In: Society ON, editor.
20. Arber DA, Orazi A, Hasserjian R, Thiele J, Borowitz MJ, Le Beau MM, et al. The 2016 revision to the World Health Organization classification of myeloid neoplasms and acute leukemia. Blood. 2016;127(20):2391-405.
21. Grunenberg A, Buske C. Monoclonal IgM Gammopathy and Waldenstrom's Macroglobulinemia. Dtsch Arztebl Int. 2017;114(44):745-51.
22. Kapoor P, Ansell SM, Fonseca R, Chanan-Khan A, Kyle RA, Kumar SK, et al. Diagnosis and Management of Waldenstrom Macroglobulinemia: Mayo Stratification of Macroglobulinemia and Risk-Adapted Therapy (mSMART) Guidelines 2016. JAMA Oncol. 2017;3(9):1257-65.
23. Mazzucchelli M, Frustaci AM, Deodato M, Cairoli R, Tedeschi A. Waldenstrom's Macroglobulinemia: An Update. Mediterr J Hematol Infect Dis. 2018;10(1):e2018004.
24. Drandi D, Genuardi E, Dogliotti I, Ferrante M, Jimenez C, Guerrini F, et al. Highly sensitive MYD88(L265P) mutation detection by droplet digital polymerase chain reaction in Waldenstrom macroglobulinemia. Haematologica. 2018;103(6):1029-37.

25. Treon SP, Xu L, Yang G, Zhou Y, Liu X, Cao Y, et al. MYD88 L265P somatic mutation in Waldenstrom's macroglobulinemia. N Engl J Med. 2012;367(9):826-33.
26. CXCR4 C-X-C motif chemokine receptor 4 [Homo sapiens (human)] 19-Mar-2019 [Available from: https://www.ncbi.nlm.nih.gov/gene/7852.
27. MYD88 MYD88 innate immune signal transduction adaptor [Homo sapiens (human)] NCBI12-Mar-2019 [Available from: https://www.ncbi.nlm.nih.gov/gene/4615.
28. Rousseau S, Martel G. Gain-of-Function Mutations in the Toll-Like Receptor Pathway: TPL2-Mediated ERK1/ERK2 MAPK Activation, a Path to Tumorigenesis in Lymphoid Neoplasms? Front Cell Dev Biol. 2016;4:50.
29. UCSC Genome Browser on Human Feb. 2009 (GRCh37/hg19) Assembly [Available from: https://genome.ucsc.edu/index.html.
30. Bonilla-Valentin FJ, Cerra J, Caceres-Perkins W, Alsina M. Case Report of IgM Multiple Myeloma: Diagnosing a Rare Hematologic Entity. Cancer Control. 2018;25(1):1073274817744448.
31. Kreitman RJ, Arons E. Update on Hairy Cell Leukemia. Clin Adv Hematol Oncol. 2018;16(3):205–15.
32. Bibi A, Java S, Chaudhar S, Joshi S, Mascerhenas R, Rabade N, et al. BRAFV600E mutation in hairy cell leukemia: A single-center experience. Indian J Pathol Microbiol. 2018 61(4):532-6.
33. Tiacci E, Trifonov V, Schiavoni G, Holmes A, Kern W, Martelli MP, et al. BRAF mutations in hairy cell leukemia. N Engl J Med. 2011;365(24):2305–15.
34. Roider T, Falini B, Dietrich S. Recent advances in understanding and managing hairy cell leukemia. F1000Research. 2018;509.
35. Tiacci E, Pettirossi V, Schiavoni G, Falini B. Genomics of Hairy Cell Leukemia. JOURNAL OF CLINICAL ONCOLOGY. 2017;35(9).
36. McCain J. The MAPK (ERK) Pathway -

Investigational Combinations for the Treatment Of BRAF-Mutated Metastatic Melanoma. P&T®. 2012;38(2).
37. Guerrini F, Paolicchi M, Ghio F, Ciabatti E, Grassi S, Salehzadeh S, et al. The Droplet Digital PCR: A New Valid Molecular Approach for the Assessment of B-RAF V600E Mutation in Hairy Cell Leukemia. Frontiers in Pharmacology. 2016;77(363).
38. De Kouchkovsky I, Abdul-Hay M. 'Acute myeloid leukemia: a comprehensive review and 2016 update'. Blood Cancer J. 2016;6(7):e441.
39. WHO - ACUTE MYELOGENOUS LEUKEMIA AND ACUTE PROMYELOCYTIC LEUKEMIA 2014 [Available from: https://www.who.int/selection_medicines/committees/expert/20/applications/AML_APL.pdf.
40. Gabert J, Beillard E, van der Velden VH, Bi W, Grimwade D, Pallisgaard N, et al. Standardization and quality control studies of 'real-time' quantitative reverse transcriptase polymerase chain reaction of fusion gene transcripts for residual disease detection in leukemia - a Europe Against Cancer program. Leukemia.2003;17(12):2318-57.
41. Control UfIC. ACUTE MYELOGENOUS LEUKEMIA AND ACUTE PROMYELOCYTIC LEUKEMIA. 2014.
42. Brunetti C, Anelli L, Zagaria A, Minervini A, Minervini CF, Casieri P, et al. Droplet Digital PCR Is a Reliable Tool for Monitoring Minimal Residual Disease in Acute Promyelocytic Leukemia. J Mol Diagn. 2017;19(3):437-44.
43. Lee GY, Christina S, Tien SL, Ghafar AB, Hwang W, Lim LC, et al. Acute promyelocytic leukemia with PML-RARA fusion on i(17q) and therapy-related acute myeloid leukemia. Cancer Genet Cytogenet. 2005;159(2):129-36.
44. PML promyelocytic leukemia [Homo sapiens (human)]: NCBI; 3-Mar-2019 [Available from: https://www.ncbi.nlm.nih.gov/gene/5371.
45. RARA retinoic acid receptor alpha [Homo sapiens (human)]: NCBI; 28-Mar-2019 [Available from: https://www.ncbi.nlm.nih.gov/gene/5914.

46. Rhinn M, Dolle P. Retinoic acid signalling during development. Development. 2012;139(5):843-58.
47. Dekking EH, van der Velden VH, Varro R, Wai H, Bottcher S, Kneba M, et al. Flow cytometric immunobead assay for fast and easy detection of PML-RARA fusion proteins for the diagnosis of acute promyelocytic leukemia. Leukemia. 2012;26(9):1976-85.
48. Lo-Coco F, Ammatuna E, Montesinos P, Sanz MA. Acute promyelocytic leukemia: recent advances in diagnosis and management. Semin Oncol. 2008;35(4):401-9.
49. Cull EH, Altman JK. Contemporary treatment of APL. Curr Hematol Malig Rep. 2014;9(2):193-201.
50. Palmirotta R, Lovero D, Cafforio P, Felici C, Mannavola F, Pelle E, et al. Liquid biopsy of cancer: a multimodal diagnostic tool in clinical oncology. Ther Adv Med Oncol. 2018;10:1758835918794630.
51. Junqueira-Neto S, Batista IA, Costa JL, Melo SA. Liquid Biopsy beyond Circulating Tumor Cells and Cell-Free DNA. Acta Cytol. 2019:1-10.
52. Chang YS, Fang HY, Hung YC, Ke TW, Chang CM, Liu TY, et al. Correlation of genomic alterations between tumor tissue and circulating tumor DNA by next-generation sequencing. Journal of Cancer Research and Clinical Oncology. 2018 Nov 1;144(11):2167-75.
53. Kubaczkova V, Vrabel D, Sedlarikova L, Besse L, Sevcikova S. Cell-free DNA - Minimally invasive marker of hematological malignancies. Eur J Haematol. 2017;99(4):291-9.
54. Messaoudi SE, Rolet F, Mouliere F, Thierry AR. Circulating cell free DNA: Preanalytical considerations. Clinica Chimica Acta. 2013 Sep 23;424:222-30.
55. Mandel P MP. Les acides nucleiques du plasma sanguin chez I' homme. C R ACAD SCI PARIS. 1948;142:241 - 3.
56. Ossandon MR, Agrawal L, Bernhard EJ, Conley BA, Dey SM, Divi RL, et al. Circulating Tumor DNA Assays in Clinical Cancer Research. J Natl Cancer Inst. 2018;110(9):929-34.
57. Lee I, Baxter D, Lee MY, Scherler K, Wang K. The Importance of Standardization on Analyzing Circulating RNA. Mol Diagn Ther. 2017;21(3):259-68.
58. Grolz D, Hauch S, Schlumpberger M, Guenther K, Voss T, Sprenger-Haussels M, et al. Liquid Biopsy Preservation Solutions for Standardized Pre-Analytical Workflows-Venous Whole Blood and Plasma. Curr Pathobiol Rep. 2018;6(4):275-86.
59. Sole C, Tramonti D, Schramm M, Goicoechea I, Armesto M, Hernandez LI, et al. The Circulating Transcriptome as a Source of Biomarkers for Melanoma. Cancers (Basel). 2019;11(1).
60. De Rubis G, Rajeev Krishnan S, Bebawy M. Liquid Biopsies in Cancer Diagnosis, Monitoring, and Prognosis. Trends Pharmacol Sci. 2019;40(3):172-86.
61. Bio-Rad. Digital Droplet PC Applications Guide.
62. Droplet Digital PCR. Aplications Guide. In: BIO-RAD, editor.
63. McCoy AM, Litterst C, Montescarlos L, Shah P, Ugozzoli L. Droplet Digital PCR: 3rd generation PCR provides improved detection, quantification, identification, and characterization of microbial targets and novel aproaches for molecular microbiology. Bio-Rad laboratories, Inc, 2000.
64. Alikian M, Whale AS, Akiki S, Piechocki K, Torrado C, Myint T, et al. RT-qPCR and RT-Digital PCR: A Comparison of Different Platforms for the Evaluation of Residual Disease in Chronic Myeloid Leukemia. Clin Chem. 2017;63(2):525-31.
65. Rustad EH, Coward E, Skytoen ER, Misund K, Holien T, Standal T, et al. Monitoring multiple myeloma by quantification of recurrent mutations in serum. Haematologica. 2017;102(7):1266-72.
66. Del Re M, Biasco E, Crucitta S, Derosa L, Rofi E, Orlandini C, et al. The Detection of Androgen Receptor Splice Variant 7 in Plasma-derived Exosomal RNA Strongly Predicts Resistance to Hormonal Therapy in Metastatic Prostate Cancer Patients. Eur Urol. 2017;71(4):680-7.

67. Nystrand CF, Ghanima W, Waage A, Jonassen CM. JAK2 V617F mutation can be reliably detected in serum using droplet digital PCR. Int J Lab Hematol. 2018;40(2):181-6.
68. Janus Serum Bank Cancer Registry in Norway2019 [Available from: https://www.kreftregisteret.no/en/Research/Janus-Serum-Bank/.
69. Technologies L. Qubit® dsDNA HS Assay Kits Catalog nos. Q32851, Q32854.
70. Castillo JJ, Hunter ZR, Yang G, Treon SP. Novel approaches to targeting MYD88 in Waldenstrom macroglobulinemia. Expert Rev Hematol. 2017;10(8):739-44.
71. Sanmamed MF, Fernandez-Landazuri S, Rodriguez C, Zarate R, Lozano MD, Zubiri L, et al. Quantitative cell-free circulating BRAFV600E mutation analysis by use of droplet digital PCR in the follow-up of patients with melanoma being treated with BRAF inhibitors. Clin Chem. 2015;61(1):297-304.
72. Lin MT, Tseng LH, Rich RG, Hafez MJ, Harada S, Murphy KM, et al. Delta-PCR, A Simple Method to Detect Translocations and Insertion/Deletion Mutations. J Mol Diagn. 2011;13(1):85-92.
73. Yuan D, Cui M, Yu S, Wang H, Jing R. Droplet digital PCR for quantification of PML-RARalpha in acute promyelocytic leukemia: a comprehensive comparison with real-time PCR. Anal Bioanal Chem. 2019;411(4):895-903.
74. Albano F, Zagaria A, Anelli L, Coccaro N, Tota G, Brunetti C, et al. Absolute quantification of the pretreatment PML-RARA transcript defines the relapse risk in acute promyelocytic leukemia. Oncotarget. 2015;6(15).
75. Aguado C, Gimenez-Capitan A, Karachaliou N, Perez-Rosado A, Viteri S, Morales-Espinosa D, et al. Fusion gene and splice variant analyses in liquid biopsies of lung cancer patients. Transl Lung Cancer Res. 2016;5(5):525-31.
76. Mihaly D, Nagy N, Papp G, Papai Z, Sapi Z. Release of circulating tumor cells and cell-free nucleic acids is an infrequent event in synovial sarcoma: liquid biopsy analysis of 15 patients diagnosed with synovial sarcoma. Diagn Pathol. 2018;13(1):81.
77. Lai J, Du B, Wang Y, Wu R, Yu Z. Next-generation sequencing of circulating tumor DNA for detection of gene mutations in lung cancer: implications for precision treatment. Onco Targets Ther. 2018;11:9111-6.

Appendix

Figure 1S

```
121  cggaaagcga aagccggcgg ggcggggcgg gtgccgcagg agaaagagga agcgctggca
181  gacaatgcga cccgaccgcg ctgaggctcc aggaccgccc gccatggctg caggaggtcc
241  cggcgcgggg tctgcggccc cggtctcctc cacatcctcc cttcccctgg ctgctctcaa
301  catgcgagtg cggcgccgcc tgtctctgtt cttgaacgtg cggacacagg tggcggccga
361  ctggaccgcg ctggcggagg agatggactt tgagtacttg gagatccggc aactggagac
421  acaagcggac cccactggca ggctgctgga cgcctggcag ggacgccctg gcgcctctgt
481  aggccgactg ctcgagctgc ttaccaagct gggccgcgac gacgtgctgc tggagctggg
541  acccagcatt gaggaggatt gccaaaagta tatcttgaag cagcagcagg aggaggctga
601  gaagccttta caggtggccg ctgtagacag cagtgtccca cggacagcag agctggcggg
661  catcaccaca cttgatgacc ccctggggca tatgcctgag cgtttcgatg ccttcatctg
721  ctattgcccc agcgacatcc agtttgtgca ggagatgatc cggcaactgg aacagacaaa
781  ctatcgactg aagttgtgtg tgtctgaccg cgatgtcctg cctggcacct gtgtctggtc
841  tattgctagt gagctcatcg aaaagaggtg ccgccggatg gtggtggttg tctctgatga
901  ttacctgcag agcaaggaat gtgacttcca gaccaaattt gcactcagcc tctctccagg
961  tgcccatcag aagcgactga tccccatcaa gtacaaggca atgaagaaag agttccccag
1021 catcctgagg ttcatcactg tctgcgacta caccaacccc tgcaccaaat cttggttctg
1081 gactcgcctt gccaaggcct tgtccctgcc ctgaagactg ttctgaggcc ctgggtgtgt
1141 gtgtatctgt ctgcctgtcc atgtacttct gccctgcctc ctcctttcgt tgtaggagga
```

Figure 46S. NM_002468.4 - 02-SEP-2018 – Isoform 2 Myd88 (canonical). Coding sequence of the mRNA of the gen Myd88. CDS (nt): 185…1114. Starting codon ATG position 185 (green); Stop coding TGA position 112 (red). In blue it is shown the codon CTG afected by the mutation, 978T>C.

Figure 2S

```
1   MRPDRAEAPG PPAMAAGGPG AGSAAPVSST SSLPLAALNM RVRRRLSLFL NVRTQVAADW
61  TALAEEMDFE YLEIRQLETQ ADPTGRLLDA WQGRPGASVG RLLELLTKLG RDDVLLELGP
121 SIEEDCQKYI LKQQQEEAEK PLQVAAVDSS VPRTAELAGI TTLDDPLGHM PERFDAFICY
181 CPSDIQFVQE MIRQLEQTNY RLKLCVSDRD VLPGTCVWSI ASELIEKRCR RMVVVVSDDY
241 LQSKECDFQT KFALSLSPGA HQKRLIPIKY KAMKKEFPSI LRFITVCDYT NPCTKSWFWT
301 RLAKALSLP
```

Figure 47S NP_002459.2 02-SEP-2018. 309 aminoacid protein. In blue its shown the starting Metionine of the protein. In red, the aminoacid Leucine at position 265. The site for the mutation L265P

Figure 3S

```
1    cgcctccctt ccccctcccc gcccgacagc ggccgctcgg gccccggctc tcggttataa
61   gatggcggcg ctgagcggtg gcggtggtgg cggcgcggag ccgggccagg ctctgttcaa
121  cggggacatg gagcccgagg ccggcgccgg cgccggcgcc gcggcctctt cggctgcgga
181  ccctgccatt ccggaggagg tgtggaatat caaacaaatg attaagttga cacaggaaca
241  tatagaggcc ctattggaca aatttggtgg ggagcataat ccaccatcaa tatatctgga
301  ggcctatgaa gaatacacca gcaagctaga tgcactccaa caaagagaac aacagttatt
361  ggaatctctg gggaacggaa ctgatttttc tgtttctagc tctgcatcaa tggataccgt
421  tacatcttct tcctcttcta gcctttcagt gctaccttca tctctttcag tttttcaaaa
481  tcccacagat gtggcacgga gcaaccccaa gtcaccacaa aaacctatcg ttagagtctt
541  cctgcccaac aaacagagga cagtggtacc tgcaaggtgt ggagttacag tccgagacag
601  tctaaagaaa gcactgatga tgagaggtct aatcccagag tgctgtgctg tttacagaat
661  tcaggatgga gagaagaaac caattggttg ggacactgat atttcctggc ttactggaga
721  agaattgcat gtggaagtgt tggagaatgt tccacttaca acacacaact ttgtacgaaa
781  aacgtttttc accttagcat tttgtgactt ttgtcgaaag ctgcttttcc agggtttccg
841  ctgtcaaaca tgtggttata aatttcacca gcgttgtagt acagaagttc cactgatgtg
901  tgttaattat gaccaacttg atttgctgtt tgtctccaag ttctttgaac accacccaat
961  accacaggaa gaggcgtcct tagcagagac tgccctaaca tctggatcat ccccttccgc
1021 acccgcctcg gactctattg ggccccaaat tctcaccagt ccgtctcctt caaaatccat
1081 tccaattcca cagcccttcc gaccagcaga tgaagatcat cgaaatcaat ttgggcaacg
1141 agaccgatcc tcatcagctc ccaatgtgca tataaacaca atagaacctg tcaatattga
1201 tgacttgatt agagaccaag gatttcgtgg tgatggagga tcaaccacag gtttgtctgc
1261 taccccccct gcctcattac ctggctcact aactaacgtg aaagccttac agaaatctcc
1321 aggacctcag cgagaaagga agtcatcttc atcctcagaa gacaggaatc gaatgaaaac
1381 acttggtaga cgggactcga gtgatgattg ggagattcct gatgggcaga ttacagtggg
1441 acaaagaatt ggatctggat catttggaac agtctacaag ggaaagtggc atggtgatgt
1501 ggcagtgaaa atgttgaatg tgacagcacc tacacctcag cagttacaag ccttcaaaaa
1561 tgaagtagga gtactcagga aaacacgaca tgtgaatatc ctactcttca tgggctattc
1621 cacaaagcca caactggcta ttgttaccca gtggtgtgag ggctccagct tgtatcacca
1681 tctccatatc attgagacca aatttgagat gatcaaactt atagatattg cacgacagac
1741 tgcacagggc atggattact tacacgccaa gtcaatcatc cacagagacc tcaagagtaa
1801 taatatattt cttcatgaag acctcacagt aaaaataggt gattttggtc tagctacagt
1861 gaaatctcga tggagtgggt cccatcagtt tgaacagttg tctggatcca ttttgtggat
1921 ggcaccagaa gtcatcagaa tgcaagataa aaatccatac agctttcagt cagatgtata
1981 tgcatttgga attgttctgt atgaattgat gactggacag ttaccttatt caaacatcaa
2041 caacagggac cagataattt ttatggtggg acgaggatac ctgtctccag atctcagtaa
2101 ggtacggagt aactgtccaa aagccatgaa gagattaatg gcagagtgcc tcaaaaagaa
2161 aagagatgag agaccactct ttccccaaat tctcgcctct attgagctgc tggcccgctc
2221 attgccaaaa attcaccgca gtgcatcaga accctccttg aatcgggctg gtttccaaac
2281 agaggatttt agtctatatg cttgtgcttc tccaaaaaca cccatccagg caggggata
2341 tggtgcgttt cctgtccact gaaacaaatg agtgagagag ttcaggagag tagcaacaaa
```

Figure 48S NM_004333.4 17-JUL-2017. Coding sequence of the mRNA of the gen BRAF. CDS (nt): 62..2362. Starting codon ATG position 62 (green); Stop coding TGA position 2362 (blue). In red it is shown the codon GTA afected by the mutation. 1799T>C

Figure 4S

```
1   MAALSGGGGG GAEPGQALFN GDMEPEAGAG AGAAASSAAD PAIPEEVWNI KQMIKLTQEH
61  IEALLDKFGG EHNPPSIYLE AYEEYTSKLD ALQQREQQLL ESLGNGTDFS VSSSASMDTV
121 TSSSSSSLSV LPSSLSVFQN PTDVARSNPK SPQKPIVRVF LPNKQRTVVP ARCGVTVRDS
181 LKKALMMRGL IPECCAVYRI QDGEKKPIGW DTDISWLTGE ELHVEVLENV PLTTHNFVRK
241 TFFTLAFCDF CRKLLFQGFR CQTCGYKFHQ RCSTEVPLMC VNYDQLDLLF VSKFFEHHPI
301 PQEEASLAET ALTSGSSPSA PASDSIGPQI LTSPSPSKSI PIPQPFRPAD EDHRNQFGQR
361 DRSSSAPNVH INTIEPVNID DLIRDQGFRG DGGSTTGLSA TPPASLPGSL TNVKALQKSP
421 GPQRERKSSS SSEDRNRMKT LGRRDSSDDW EIPDGQITVG QRIGSGSFGT VYKGKWHGDV
481 AVKMLNVTAP TPQQLQAFKN EVGVLRKTRH VNILLFMGYS TKPQLAIVTQ WCEGSSLYHH
541 LHIIETKFEM IKLIDIARQT AQGMDYLHAK SIIHRDLKSN NIFLHEDLTV KIGDFGLATV
601 KSRWSGSHQF EQLSGSILWM APEVIRMQDK NPYSFQSDVY AFGIVLYELM TGQLPYSNIN
661 NRDQIIFMVG RGYLSPDLSK VRSNCPKAMK RLMAECLKKK RDERPLFPQI LASIELLARS
721 LPKIHRSASE PSLNRAGFQT EDFSLYACAS PKTPIQAGGY GAFPVH
```

Figure 49S NP_004324.2 02-MAY-2019. 766 aminoacid protein. In blue its shown the starting Metionine of the protein. In red, the aminoacid Valine at position 600. The site for the mutation V600E

Figure 5S

Agilent result of 10 ctDNA samples tested. Patient 1, 2, 4, 7 and 9-2 showed a predominant pick at 150 base pars, corresponding with ctDNA fragment. However, patient 9-5, 9-6, 9-8 and patient 11 showed high picks at bigger sizes suggesting that it could be either genomic contamination of ctDNA fragments of bigger size.

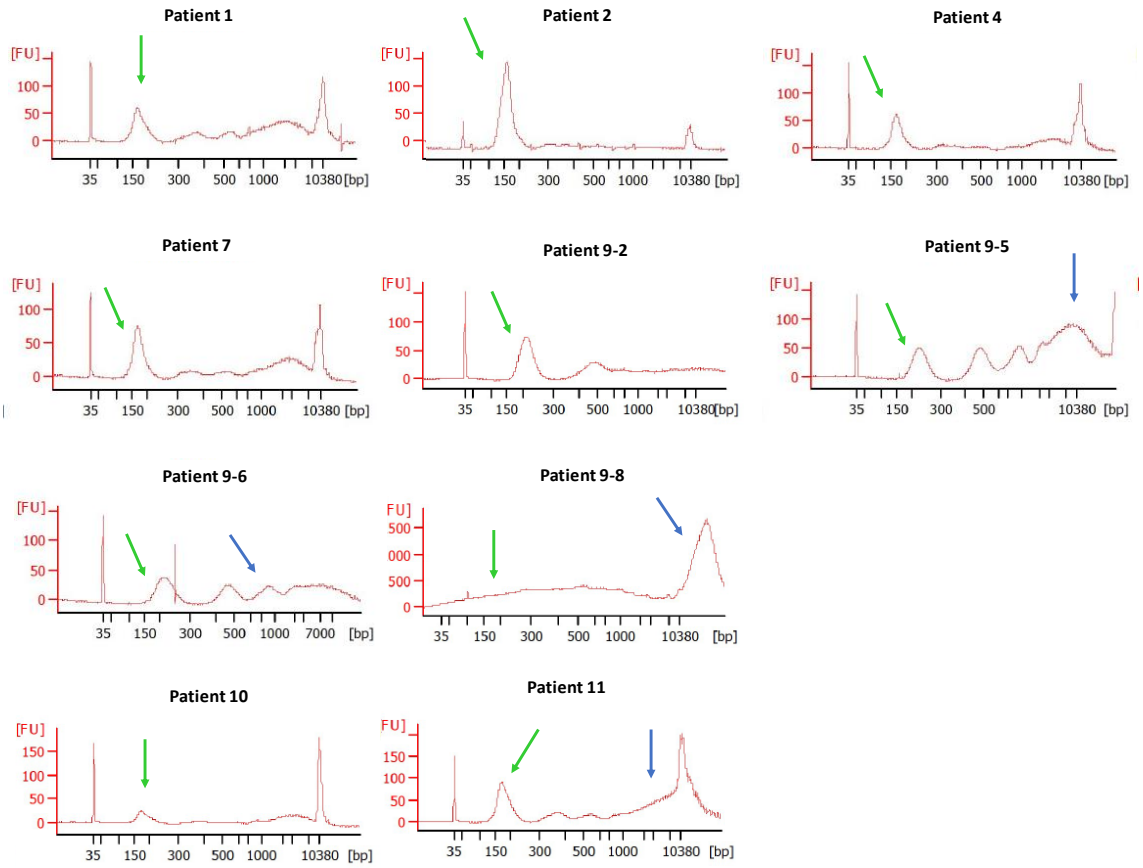

Figure 50S Agilent chip results. Fluorescence vs base pairs. Green arrow shows the cfDNA pick at 150-200 base pairs. Blue arrow shows other DNA fragments at 10300 base pairs

Figure 6S

Sequence of the Gene Block used as positive control for Myd88 L265P

CTTAGATGGGGGATGGCTGTTGTTAACCCTGGGGTTGAAGACTGGGCTTGTCCCACCATGGG
GCAAGGGCCTGATGCCAGCATGGCACCCCTTGGCTTGCAGGTGCCCATCAGAAGCGACCGAT
CCCCATCAAGTACAAGGCAATGAAGAAAGAGTTCCCCAGCATCCTGAGGTTCATCACTGTCTG
CGACTACACCAACCCCTGCACCAAATCTTGGTTCTGGACTCGCCTTGCCAAGGCCTTGTCCCTG

Figure 7S

Bcr1_2 Gene block

CAGCCCAGGCCCAGCACCTCCAAGGCAGTCTCACCACCCCACCTGGATGGACCGCCTAGCCCC
AGGAGCCCCGTCATAGGAAGTGAGGTCTTCCTGCCCAACAGCAACCACGTGGCCAGTGGCGC
CGGGGAGGCAGCATTGAGACCCAGAGCAGCAGTTCTGAAGAGATAGTGCCCAGCCCTCCCTC
GCCACCCCCTCTACCCCGCATCTACAAGCCTTGCTTTGTCTGTCAGGACAAGTCCTCAGGCTAC

Bcr3 Gene block

TTTCCTGCGCCAGGCGCTCTGCCGCCTGCGCCAGGAGGAGCCCCAGAGCCTGCAAGCTGCCG
TGCGCACCGATGGCTTCGACGAGTTCAAGGTGCGCCTGCAGGACCTCAGCTCTTGCATCACCC
AGGGCATTGAGACCCAGAGCAGCAGTTCTGAAGAGATAGTGCCCAGCCCTCCCTCGCCACCCC
CTCTACCCCGCATCTACAAGCCTTGCTTTGTCTGTCAGGACAAGTCCTCAGGCTACCACTATG

Figure 51S Sequence of the gBlock. In grey it is shown the sequence of the forward and revers primer (its represented the sequence of the complementary revers primer). In blue the sequence of the probe (FAM).

Figure 8S

Limit of Detection test for Myd88 L265P. Four serial dilutions 1:10 were performed to reach 1:10000. The obtained regression line showed a good linearity R^2=0,93 and a huge similarity with the one obtained theoretically, however, when it comes to the last two dilutions – 1:1000 and 1:10000 the linearity decrease suggesting that, a low abundance of the molecule in a highly WT background may affect the accurate detection of the mutated molecules. The number of copies detected in the dilution 1:1000 was 0,6 copies/reaction, meanwhile the positive control for the same dilution showed a concentration of 3,2 copies per reaction. Theoretically, that dilution had 3 copies in the reaction. This result suggests that in this experiment, the ddPCR is able to detect low copy number but it can't detect it when those molecules are in a highly WT constant background.

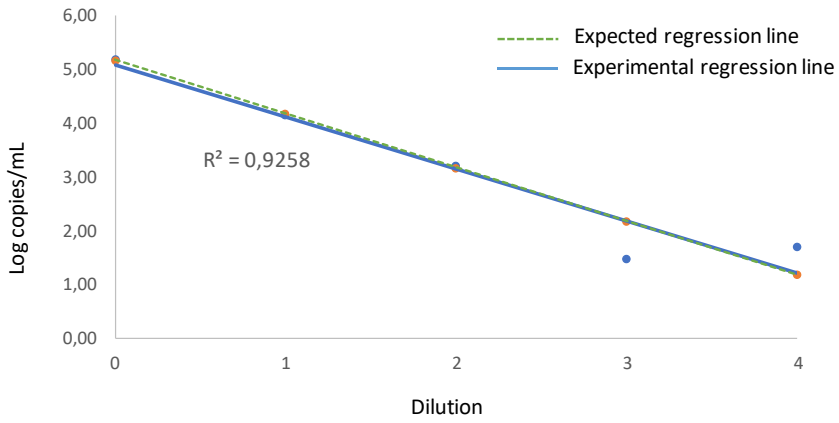

Figure 8S LoD for Myd88 assay. Seral dilutions 1:10. a) Log_{10} of the mutated concentration (copy number per µL of ddPCR reaction) plotted against the corresponding dilutions. The curve is transformed into a linear regression model being R^2= 0,93. **b)** Expected and experimental results for the different dilutions. *shows the dilution that does not follow the linear regression.

Figure 9S

Red circle shown the IgM value at the time of the serum sample

Patient 1

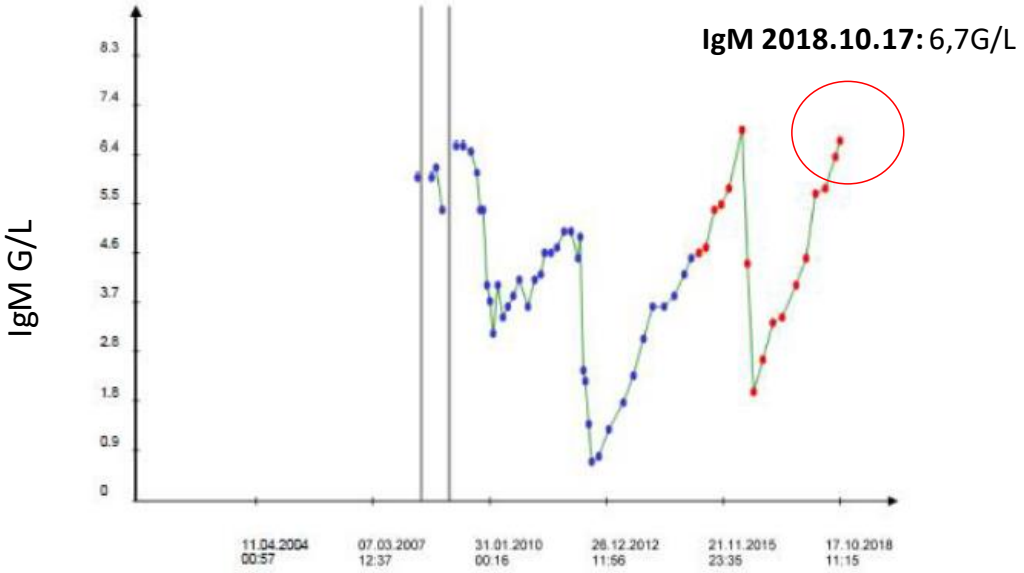

Patient 2

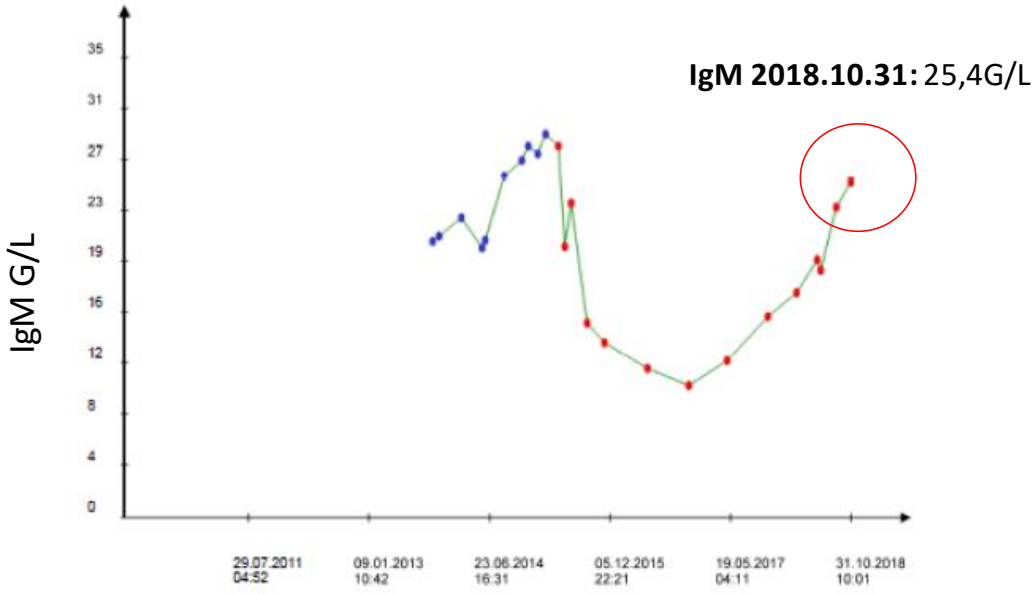

Patient 3

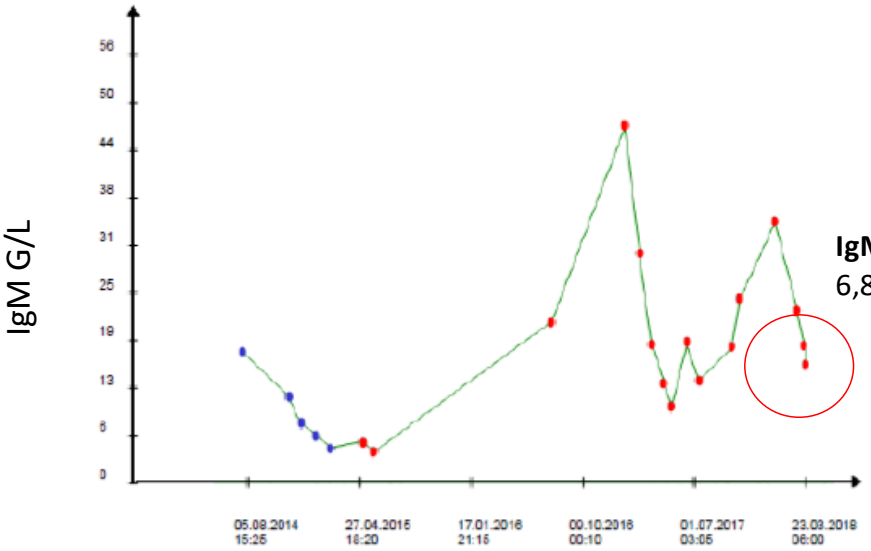

IgM 2018.01.09:
6,8G/L

Patient 4

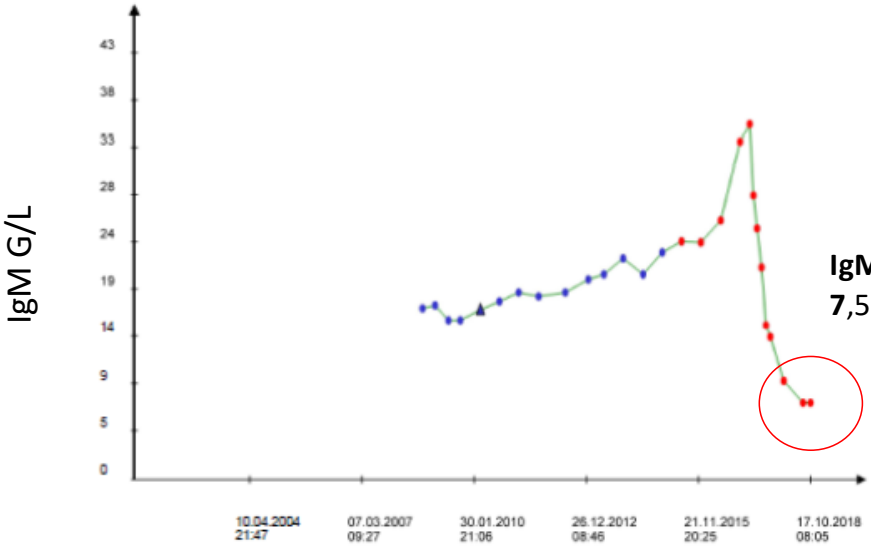

IgM 2018.10.17:
7,5G/L

Patient 5

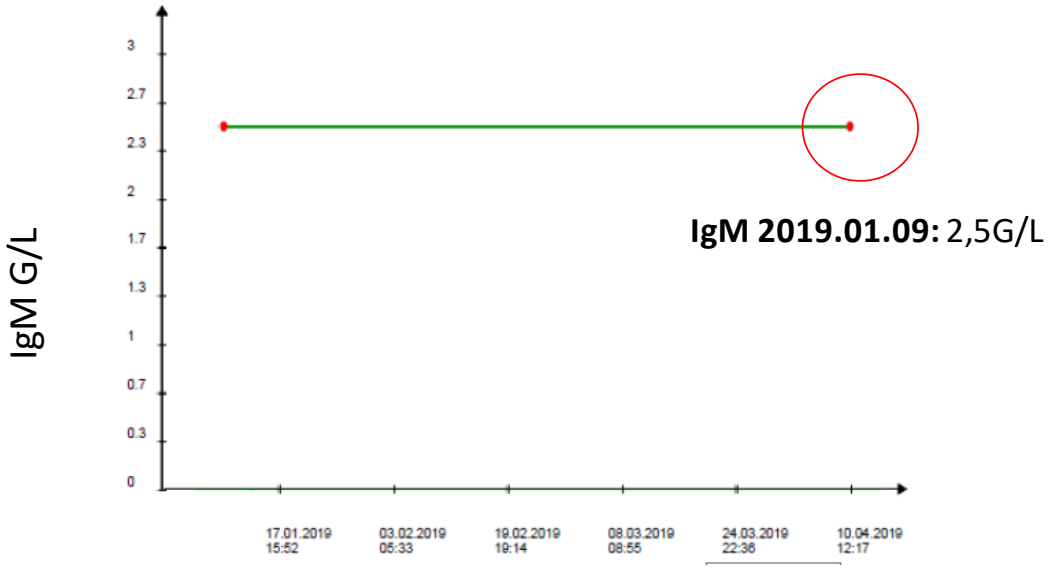

IgM 2019.01.09: 2,5G/L

Patient 6

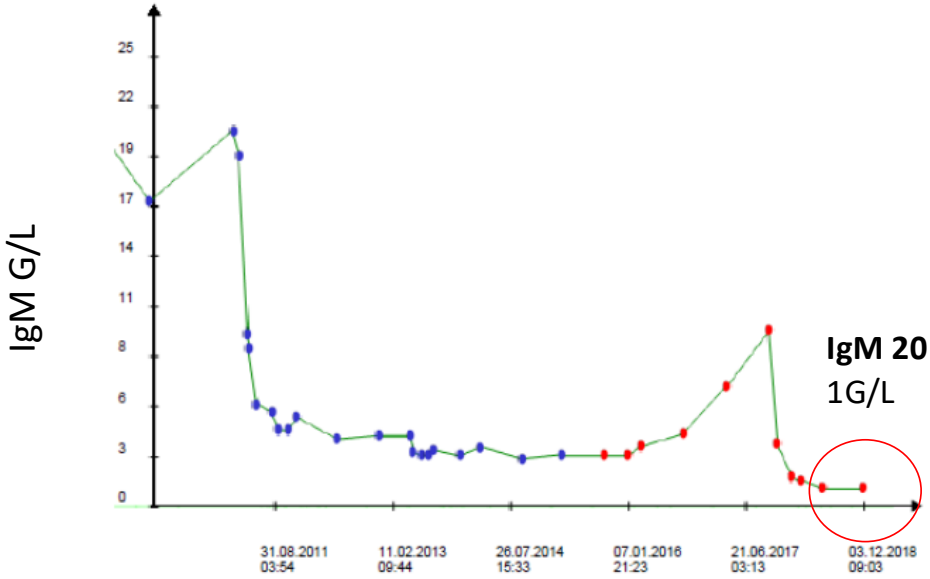

IgM 2018.12.03: 1G/L

Patient 7

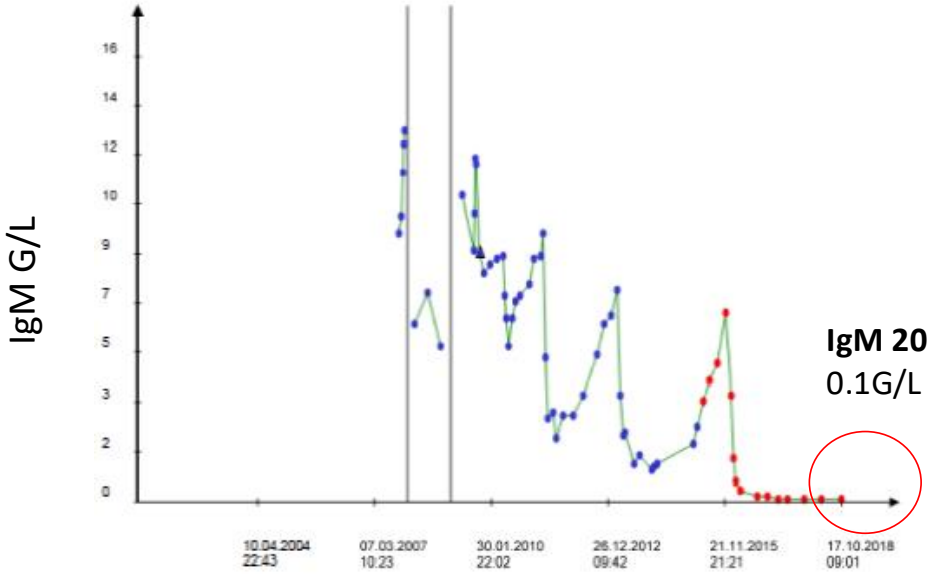

IgM 2018.10.17:
0.1G/L

Patient 8

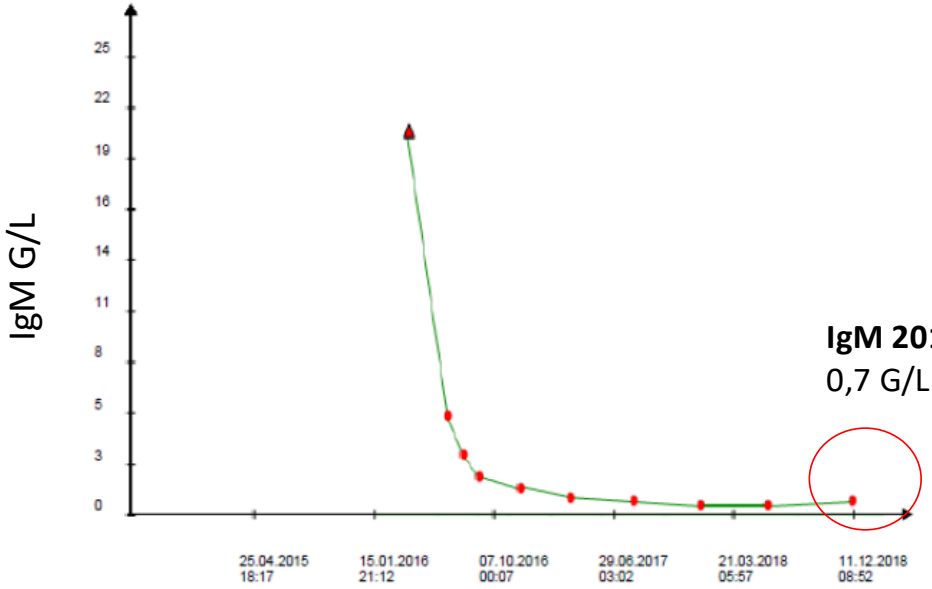

IgM 2018.12.03:
0,7 G/L

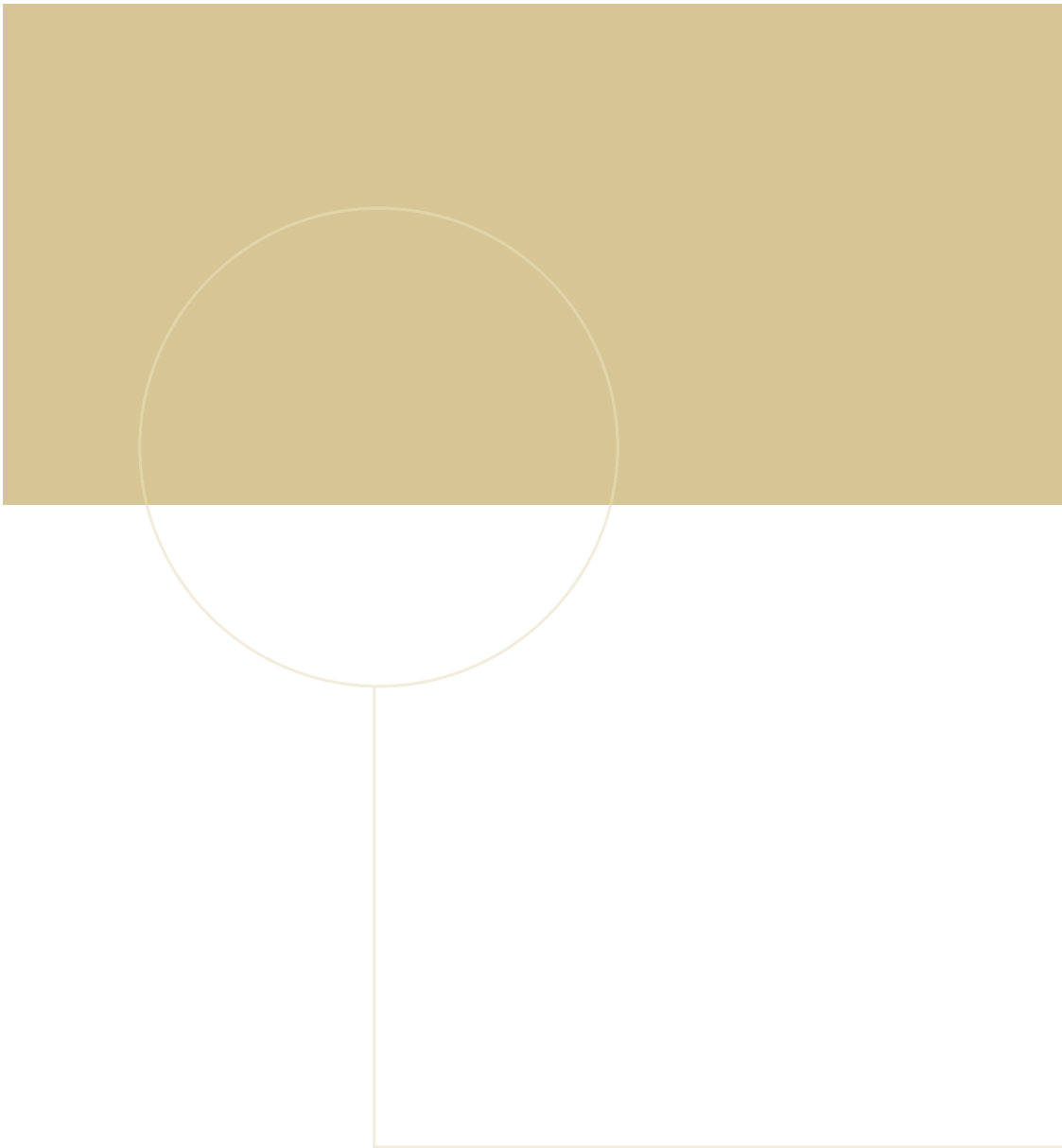

NTNU
Norwegian University of
Science and Technology